

Holographic and massive pair plasma state in Friedman Universe: baryogenesis, magnetogenesis, and dark-matter wave

She-Sheng Xue

ICRANet Piazzale della Repubblica, 10 -65122, Pescara, Italy
Physics Department, Sapienza University of Rome, Rome, Italy
INFN, Sezione di Perugia, Perugia, Italy
ICTP-AP, University of Chinese Academy of Sciences, Beijing, China
E-mail: xue@icra.it and shesheng.xue@gmail.com

Abstract. Quantum massive particle and antiparticle pair production and oscillation result in a holographic and massive pair plasma state in reheating. Particle and antiparticle densities perturbations in the plasma form the acoustic waves of particle-antiparticle symmetric and asymmetric densities. We derive wave equations and find frequencies of the lowest-lying perturbation modes (zero wave number). Comparing their sizes with the horizon, we show the superhorizon crossing at reheating. It accounts for baryogenesis and magnetogenesis. The obtained baryon number-to-entropy ratio and primordial magnetic field upper and lower limits agree with observations. Moreover, we study the physically interested perturbation modes (nonzero wave number) that represent dark-matter acoustic waves. These modes exited from the horizon and returned to the horizon after the recombination. Thus, they possibly imprint on the matter power spectrum at large length scales and have physical influences on the formation of large-scale structures and galaxies.

Contents

1	Introduction	2
2	Particle and antiparticle oscillating perturbations	3
2.1	Particle and anti-particle density perturbations	4
2.1.1	Continuity and Eulerian equations of particles	4
2.1.2	Density perturbations of particles and antiparticles	4
2.2	Symmetric and asymmetric density perturbations	5
2.2.1	Acoustic wave equations for density perturbations	5
2.2.2	Oscillating equations of lowest-lying modes	6
3	Particle-antiparticle asymmetry and horizon crossing	7
3.1	Under- and over-damped oscillating modes	7
3.2	Lowest-lying mode crossing horizon	8
3.3	Symmetric and asymmetric oscillating amplitudes at horizon crossing	9
3.3.1	Lowest-lying mode amplitudes at horizon crossing	9
3.3.2	Particle-antiparticle asymmetry due to horizon crossing	10
4	Horizon crossings at reheating start and end	10
4.1	Subhorizon crossing in preheating \mathcal{P} -episode	11
4.1.1	Particle-antiparticle asymmetry in pre-inflation and inflation	11
4.1.2	Particle-antiparticle symmetry in \mathcal{M} -episode	11
4.1.3	Subhorizon crossing and particle-antiparticle symmetry	12
4.2	Superhorizon crossing in genuine reheating \mathcal{R} -episode	13
4.2.1	Superhorizon crossing in reheating	13
4.2.2	Initial particle-antiparticle asymmetry for standard cosmology	14
5	Baryogenesis and magnetogenesis in reheating epoch	15
5.1	Origin of net baryon numbers	16
5.2	Baryon number-to-entropy ratio	17
5.3	Magnetogenesis via baryogenesis	17
5.3.1	Upper limit of primordial magnetic fields	18
5.3.2	Lower limit of primordial magnetic fields	19
6	Dark-matter acoustic wave and large-scale structure	20
6.1	Pair-density and particle-antiparticle-density perturbations	21
6.2	Pair-density perturbation and large-scale structure	22
6.2.1	Subhorizon stable modes and dark-matter acoustic waves	22
6.2.2	Unstable superhorizon modes and large-scale structure	23
6.3	Particle-antiparticle density perturbations and “plasma” acoustic wave	25
7	Summary and remarks	26

1 Introduction

In the standard model of modern cosmology (Λ CDM), the cosmological constant (dark energy), inflation, reheating, dark matter and coincidence problem have been long-standing basic issues for decades. The inflation [1–7] and reheating [8–17] are the fundamental epochs lead to the hot Big Bang of standard cosmology. The cosmic microwave background (CMB) observations have been attempting to determine a unique model of inflation and reheating. In addition, two important observations of the baryon and anti-baryon asymmetry and primordial magnetic fields call for understanding baryogenesis and magnetogenesis. We recall that in the Standard Model (SM) of elementary particle physics, it is difficult to have baryogenesis in agreement with the baryon number-to-entropy ratio $n_B/s = 0.864_{-0.015}^{+0.016} \times 10^{-10}$ [18]. Particle physicists have proposed many ideas for baryon asymmetry with ingredients beyond SM [19–22]. Some interesting connections between reheating and baryogenesis have been studied [23–34]. On the other hand, magnetic fields have been observed in galaxies $B_{10-10^2\text{kpc}} \sim 10^{-5}\text{G}$ and galaxy clusters $B_{0.1-1\text{Mpc}} \sim 10^{-6}\text{G}$. There is a (conservative) lower bound on the strength of magnetic fields with cosmic scale correlation lengths $B_{>1\text{Mpc}} > 10^{-17}\text{G}$ [35]. CMB observations have put upper bounds on it $B_{1\text{Mpc}} < 10^{-9}\text{G}$ [36]. Many ideas and efforts are advanced to understand the primordial origin of these magnetic fields [37–41]. We attempt to study these issues in the $\tilde{\Lambda}$ CDM scenario, which has two main features.

First, a time-varying cosmological $\tilde{\Lambda}$ term in the Friedman equation represents such interacting dark energy with matter and radiation. The Friedman equations for a flat Universe of horizon H are [42]

$$H^2 = \frac{8\pi G}{3}\rho; \quad \dot{H} = -\frac{8\pi G}{2}(\rho + p), \quad (1.1)$$

where energy density $\rho \equiv \rho_M + \rho_R + \rho_\Lambda$ and pressure $p \equiv p_M + p_R + p_\Lambda$, and Equation of State $p_{M,R,\Lambda} = \omega_{M,R,\Lambda}\rho_{M,R,\Lambda}$. The second Equation of (1.1) is the generalised conservation law (Bianchi identity) for including time-varying cosmological term (dark energy) $\rho_\Lambda(t) \equiv \tilde{\Lambda}/(8\pi G)$. It reduces to the usual equation $\dot{\rho}_M + (1 + \omega_M)H\rho_M + \dot{\rho}_R + (1 + \omega_R)H\rho_R = 0$ for time-constant ρ_Λ .

Second, a holographic and massive pair plasma state creates due to pair production [43] and oscillation [44] of the large number and massive particles and anti-particles, for details see Secs. 3-4 of Ref. [45]. We describe such a state as a perfect fluid state of effective number n_M^H and energy ρ_M^H densities of massive stable and unstable pairs,

$$\rho_M^H \equiv 2\chi m^2 H^2, \quad n_M^H \equiv \chi m H^2. \quad (1.2)$$

The equation of state and pressure $p_M^H = \omega_M^H \rho_M^H$. The lower limit $\omega_M^H \approx 0$ for $m \gg H$, and the upper limit $\omega_M^H \lesssim 1/3$ for $m \gtrsim H$. The m is the mass parameter of the massive pair plasma state, and we will specify it as \hat{m} for the reheating epoch. The massive pair plasma state is a holographic layer near the horizon. The layer width $\lambda_m = (\chi m)^{-1} \ll H^{-1}$ and the width parameter $\chi \ll 1$. The introduced average rate

Γ_M

$$\Gamma_M \approx \frac{\chi \hat{m}}{4\pi} \epsilon, \quad \tau_M = \Gamma_M^{-1}, \quad (1.3)$$

and time scale τ_M effectively describe how the pair plasma state varies in time, as the Universe's horizon H evolves. The Universe evolution ϵ -rate is defined as,

$$\epsilon \equiv -\frac{\dot{H}}{H^2} = \frac{3}{2} \frac{(1 + \omega_M)\rho_M + (1 + \omega_R)\rho_R}{\rho_\Lambda + \rho_M + \rho_R}. \quad (1.4)$$

The second equation comes from the Friedman equations (1.1). The pair plasma state (1.2) contributes to the Friedman equation (1.1) via the cosmic rate equation of Boltzmann type,

$$\dot{\rho}_M + 3(1 + \omega_M)H\rho_M = \Gamma_M(\rho_M^H - \rho_M) - \Gamma_M^{\text{de}}\rho_M, \quad (1.5)$$

where Γ_M^{de} and $\tau_R = (\Gamma_M^{\text{de}})^{-1}$ are unstable massive pair decay rate and time. For details, see Secs. 4-5 of Ref. [45].

In such $\tilde{\Lambda}$ CDM scenario, we have studied singularity-free and large-scale anomaly issues, the spectral index and tensor-to-scalar ratio relation in the inflation epoch [44], and calculated reheating energy and entropy, and cold dark matter in the reheating epoch [45]. The results are consistent with observations. Based on these studies and results, we turn to investigate baryogenesis and magnetogenesis in the reheating epoch in the present article.

In Sec. 2, we describe the particle-antiparticle symmetric and asymmetric density perturbations and derive their acoustic wave equations. We analyse their acoustic wavelengths in Sec. 3 and discuss their horizon crossings that cause particle-antiparticle asymmetry in Sec. 4. We calculate the baryon number-to-entropy ratio and primordial magnetic field in Sec. 5. In addition, following the preliminary studies of dark matter wave [44], we present in Sec. 6 the studies of the dark-matter acoustic waves for a given comoving wavelength and their relevances to physical observations and effects at large-distance scales. In this article, $G = M_{\text{pl}}^{-2}$ is the Newton constant, M_{pl} is the Planck scale and reduced Planck scale $m_{\text{pl}} \equiv (8\pi)^{-1/2} M_{\text{pl}} = 2.43 \times 10^{18} \text{GeV}$.

2 Particle and antiparticle oscillating perturbations

The massive pair plasma density (1.2) contains the same numbers of particles F and antiparticles \bar{F} , and the net particle number is precisely zero. The particle and antiparticle symmetry holds for the local particle-number equipartition or chemical equilibrium at the time scale τ_M . It differs from the time scale $\tau_H = H^{-1}$ of the horizon evolution. This difference possibly makes some physical consequences of particle and antiparticle density perturbations. We attempt to present a detailed analysis of these aspects.

2.1 Particle and anti-particle density perturbations

Separating particles from antiparticles in the massive pair plasma state (1.2), we study their density perturbations, respectively, and examine symmetric and asymmetric density perturbations of particles and antiparticles.

2.1.1 Continuity and Eulerian equations of particles

Analogously to the study of cosmic perturbation, see for example [46], the linear perturbations of massive particles and antiparticles are separately studied by using their continuity equation and Eulerian equations of Newtonian motion describing two perfect fluids of particle (+) and antiparticle (-) densities $\rho_M^\pm(t, \mathbf{x})$, pressures $p_M^\pm(t, \mathbf{x})$ and velocities $\mathbf{v}_M^\pm(t, \mathbf{x})$ in the Robertson-Walker space-time (Freemmann Universe)

$$\dot{\rho}_M^\pm + \nabla \cdot (\rho_M^\pm \mathbf{v}_M^\pm) = \Gamma_M(\rho_M^0 - \rho_M^\pm) - \Gamma_M^{\text{de}} \rho_M^\pm, \quad (2.1)$$

$$\dot{\mathbf{v}}_M^\pm + (\mathbf{v}_M^\pm \cdot \nabla) \mathbf{v}_M^\pm = -(\rho_M^\pm)^{-1} \nabla p_M^\pm - \nabla \Phi, \quad (2.2)$$

$$\nabla^2 \Phi = 4\pi G(\rho_M^+ + \rho_M^-), \quad (2.3)$$

$$\rho_M^0 = (1/2)\rho_M^H = \chi \hat{m}^2 H^2, \quad (2.4)$$

and the last line ρ_M^0 is the unperturbed mean density. In Eq. (2.1), we use the detailed balance term $\Gamma_M(\rho_M^0 - \rho_M^\pm)$ to describe fluctuating densities ρ_M^\pm around the mean density with the time scale $\tau_M = \Gamma_M^{-1}$. The term $\Gamma_M^{\text{de}} \rho_M^\pm$ describes unstable massive pair decay of the time scale $\tau_R = (\Gamma_M^{\text{de}})^{-1}$. The arguments in the above equations are comoving coordinates (\mathbf{x}, \mathbf{k}) and the time derivative and space gradients are taken with respect to the physical coordinates $(a\mathbf{x}, \mathbf{k}/a)$. The zeroth order solutions ρ_M^\pm to Eqs. (2.1,2.2,2.3) are the density ρ_M^0 of massive pair plasma, which follows the Hubble flow $\mathbf{v}_M^0 = d(a\mathbf{x})/dt = H a \mathbf{x}$, and gives the gravitational potential $\Phi^0 = (2\pi G/3)\rho_M^0 |\mathbf{x}|^2$.

The interacting rates Γ_M and Γ_M^{de} , the gravitational potential Φ and mean density $\rho_M^0 = (1/2)\rho_M^H$ are invariant under the particle and antiparticle transformation. Therefore, Equations (2.1-2.4) fully respect the symmetry of particle and antiparticle. We will neglect the decay term $\Gamma_M^{\text{de}} \rho_M^\pm$ by considering $\Gamma_M \gg \Gamma_M^{\text{de}}$, namely, the massive pair plasma density variation rate is much larger than unstable pair decay rate. The reason will be given later in Fig. 1 caption. One should distinguish the continuum equation (2.1) from the cosmic rate equation (1.5). The former is the equation for particle (antiparticle) density perturbations inside the massive pair plasma. The latter is the equation for the massive pair plasma density interacting with the matter density in the Friedman equation.

2.1.2 Density perturbations of particles and antiparticles

Here the usual approach of density perturbation is adopted for analysis. We consider the small perturbations around the averaged values ρ_M^0 and \mathbf{v}_M^0 of massive pair plasma by writing

$$\delta \mathbf{v}_M^\pm = \mathbf{v}_M^\pm - \mathbf{v}_M^0, \quad \delta \rho_M^\pm = \rho_M^\pm - \rho_M^0 \quad \text{and} \quad \delta_M^\pm = \delta \rho_M^\pm / \rho_M^0. \quad (2.5)$$

Up to the first order in the perturbative quantities, Equations (2.1), (2.2) and (2.3) become

$$d(\delta\rho_M^\pm)/dt + \rho_M^0 \nabla \cdot (\delta\mathbf{v}_M^\pm) + 3H\delta\rho_M^\pm = -\Gamma_M\delta\rho_M^\pm, \quad (2.6)$$

$$d(\delta\mathbf{v}_M^\pm)/dt + H\delta\mathbf{v}_M^\pm = -(\rho_M^0)^{-1}\nabla\delta p_M^\pm - \nabla\delta\Phi, \quad (2.7)$$

and the Poisson equation becomes

$$\nabla^2\delta\Phi = 4\pi G(\delta\rho_M^+ + \delta\rho_M^-). \quad (2.8)$$

In terms of $\delta_M^\pm = \delta\rho_M^\pm/\rho_M^0$, Equation (2.6) yields

$$\nabla \cdot \delta\mathbf{v}_M^\pm = -(\dot{\delta}_M^\pm + \Gamma_M\delta_M^\pm). \quad (2.9)$$

Taking the gradient of Eq. (2.7), we arrive at

$$\ddot{\delta}_M^\pm + (\Gamma_M + 2H)\dot{\delta}_M^\pm + (2H\Gamma_M + \dot{\Gamma}_M)\delta_M^\pm = v_s^2\nabla^2\delta_M^\pm + 4\pi G\rho_M^0(\delta_M^+ + \delta_M^-) \quad (2.10)$$

where the sound velocity

$$v_s = (\delta p_M^\pm/\delta\rho_M^\pm)^{1/2}. \quad (2.11)$$

Equation (2.10) represents the perturbations of particle and antiparticle densities. It reduces to the usual equation for density perturbation in the case $\Gamma_M = 0$ and $\dot{\Gamma}_M = 0$.

2.2 Symmetric and asymmetric density perturbations

Moreover, to describe the perturbation of the symmetric particle-antiparticle pair density, and the perturbation of the asymmetrical particle-antiparticle density we introduce:

$$\Delta_M \equiv (\delta_M^+ + \delta_M^-)/2 = (\rho_M^{+-} - \rho_M^H)/\rho_M^H, \quad (2.12)$$

$$\delta_M \equiv (\delta_M^+ - \delta_M^-)/2 = (\rho_M^+ - \rho_M^-)/\rho_M^H, \quad (2.13)$$

where the sum $\rho_M^{+-} \equiv \rho_M^+ + \rho_M^-$. Henceforth, we call Δ_M the pair-density ρ_M^{+-} perturbation and δ_M the particle-antiparticle-density perturbation.

2.2.1 Acoustic wave equations for density perturbations

Replacing Eqs. (2.12,2.13) in Eq. (2.10), we obtain acoustic wave equations for the density perturbations δ_M and Δ_M ,

$$\ddot{\delta}_M + (\Gamma_M + 2H)\dot{\delta}_M + (2H\Gamma_M + \dot{\Gamma}_M)\delta_M = v_s^2\nabla^2\delta_M, \quad (2.14)$$

$$\ddot{\Delta}_M + (\Gamma_M + 2H)\dot{\Delta}_M + (2H\Gamma_M + \dot{\Gamma}_M)\Delta_M = v_s^2\nabla^2\Delta_M + 4\pi G\rho_M^H\Delta_M. \quad (2.15)$$

It is shown that the modes Δ_M and δ_M satisfy the same type of oscillating equation, except an additional term $4\pi G\rho_M^H\Delta_M$ in Eq. (2.15) due to massive pairs in the external gravitational potential. In the inflation epoch and the \mathcal{M} -episode, the ϵ -rate

(1.4) varies slowly in time, we approximately neglect $\dot{\Gamma}_M = (\chi\hat{m}/4\pi)\dot{\epsilon} \gtrsim 0$. In brief transitions \mathcal{P} -episode and \mathcal{R} -episode, ϵ variation is large. For details, see Sec. 7 and Fig. 3 (d) of Ref. [45].

Furthermore, we define the Fourier transformation from $f_M(\mathbf{x}, t) = \Delta_M(\mathbf{x}, t), \delta_M(\mathbf{x}, t)$ to \mathbf{k} modes $f_M^{\mathbf{k}}(t) = \Delta_M^{\mathbf{k}}(t), \delta_M^{\mathbf{k}}(t)$,

$$f_M(\mathbf{x}, t) = \frac{1}{V_{\text{pair}}^{1/2}} \sum_{\mathbf{k}} f_M^{\mathbf{k}}(t) e^{i\mathbf{k}\mathbf{x}}, \quad (2.16)$$

$$f_M^{\mathbf{k}}(t) = \frac{1}{V_{\text{pair}}^{1/2}} \int d^3x f_M(\mathbf{x}, t) e^{-i\mathbf{k}\mathbf{x}}, \quad (2.17)$$

where V_{pair} is the spatial physical volume of massive pair plasma. The corresponding wave-propagating equations for \mathbf{k} -modes' $\delta_M^{\mathbf{k}}$ and $\Delta_M^{\mathbf{k}}$ read,

$$\ddot{\delta}_M^{\mathbf{k}} + (\Gamma_M + 2H)\dot{\delta}_M^{\mathbf{k}} + 2H\Gamma_M\delta_M^{\mathbf{k}} = -(v_s^2|\mathbf{k}|^2/a^2)\delta_M^{\mathbf{k}} \quad (2.18)$$

$$\ddot{\Delta}_M^{\mathbf{k}} + (\Gamma_M + 2H)\dot{\Delta}_M^{\mathbf{k}} + 2H\Gamma_M\Delta_M^{\mathbf{k}} = -(v_s^2|\mathbf{k}|^2/a^2)\Delta_M^{\mathbf{k}} + 4\pi G\rho_M^H\Delta_M^{\mathbf{k}}. \quad (2.19)$$

These are semi-classical equations governing the oscillating modes $\delta_M^{\mathbf{k}}$ and $\Delta_M^{\mathbf{k}}$ of frequencies

$$\omega_\delta^2(\mathbf{k}) = 2H\Gamma_M + (v_s^2|\mathbf{k}|^2/a^2) \quad (2.20)$$

$$\omega_\Delta^2(\mathbf{k}) = 2H\Gamma_M + (v_s^2|\mathbf{k}|^2/a^2) - 4\pi G\rho_M^H. \quad (2.21)$$

The Γ_M -term contributes to the friction coefficient $(\Gamma_M + 2H)$ in oscillation equations and ‘‘quasi mass’’ term $(2H\Gamma_M)^{1/2}$ in the oscillation frequency $\omega_{\delta,\Delta}^2(\mathbf{k})$.

The term $4\pi G\rho_M^H$ in Eqs. (2.19,2.21) could lead to the Jeans instability, because of the gravitational attraction of massive pair plasma. Observe that in Eq. (2.21) $4\pi G\rho_M^H = 8\pi\chi(m/M_{\text{pl}})^2H^2$ is much smaller than $2H\Gamma_M + (v_s^2|\mathbf{k}|^2/a^2)$ even for the case $|\mathbf{k}| = 0$ and $m \gg H$ ($v_s^2 \ll 1$) in the inflation and reheating epochs, as well as standard cosmology. Therefore the negative term $4\pi G\rho_M^H$ can be neglected and $\omega_\Delta^2(\mathbf{k}) > 0$, implying the Jeans instability should not occur in these epochs.

2.2.2 Oscillating equations of lowest-lying modes

We will discuss the solutions to Eqs. (2.18-2.21) for the density perturbations in the inflation epoch and three episodes \mathcal{P} , \mathcal{M} and \mathcal{R} of the reheating epoch ($m \rightarrow \hat{m}$). We first focus on the lowest-lying oscillation modes by neglecting the pressure term $v_s^2\nabla^2$ or $(v_s^2|\mathbf{k}|^2/a^2)$ terms for wave propagation, since pairs are massive ($\hat{m} \gg H$) and their sound velocity is small $v_s^2 \ll 1$. Equations (2.18-2.21) become oscillating equations,

$$\ddot{\delta}_M^0 + (\Gamma_M + 2H)\dot{\delta}_M^0 + 2H\Gamma_M\delta_M^0 = 0, \quad (2.22)$$

$$\ddot{\Delta}_M^0 + (\Gamma_M + 2H)\dot{\Delta}_M^0 + 2H\Gamma_M\Delta_M^0 = 0, \quad (2.23)$$

where the lowest lying oscillation modes $\delta_M^0 \equiv \delta_M^{\mathbf{k}=\mathbf{0}}$ and $\Delta_M^0 \equiv \Delta_M^{\mathbf{k}=\mathbf{0}}$ with the frequencies $\omega_\delta \equiv \omega_\delta(|\mathbf{k}| = \mathbf{0})$ and $\omega_\Delta \equiv \omega_\Delta(|\mathbf{k}| = \mathbf{0})$,

$$\omega_\delta^2 = \omega_\Delta^2 = 2H\Gamma_M. \quad (2.24)$$

We call the lowest-lying modes as “zero modes” Δ_M^0 and δ_M^0 of pair-density and particle-antiparticle-density oscillations. We stress that in this semi-classical approximation frequency (2.24) of these zero modes weakly depend on the time t in the period of slowly time-varying H and Γ_M under consideration.

To end this section, we would like to mention that the oscillations δ_M^0 are the spatial fluctuations in the number of particles or antiparticles (compositions) per co-moving volume, and the oscillations Δ_M^0 are the spatial fluctuations in the number of pairs per co-moving volume.

3 Particle-antiparticle asymmetry and horizon crossing

In general, we expect that for large frequencies $\omega_{\delta,\Delta} \gg (\Gamma_M + 2H)$, the modes δ_M^0 and Δ_M^0 are underdamped oscillating inside the horizon. While small frequencies $\omega_{\delta,\Delta} \ll (\Gamma_M + 2H)$, the friction term $(\Gamma_M + 2H)\dot{\delta}_M^0$ dominates, the amplitudes of the modes δ_M^0 and Δ_M^0 are overdamped and frozen to be constants outside the horizon. Following the usual approach, we present a quantitative analysis to show this phenomenon by using the simplified Eqs. (2.22,2.23) and (2.24) in one dimension and assuming isotropic tree-dimension oscillations.

In terms of dimensionless variables $t \rightarrow \hat{m}t$, $\Gamma_M \rightarrow \Gamma_M/\hat{m}$ and $H \rightarrow H/\hat{m}$, we rewrite Eq. (2.22) in the form of the usual equation for a spherical harmonic oscillator in three dimensions,

$$\ddot{\delta}_M^0 + 2\zeta\omega_\delta\dot{\delta}_M^0 + \omega_\delta^2\delta_M^0 = 0, \quad (3.1)$$

and the same for the mode Δ_M^0 . The underdamped frequency ω_δ and the damping ratio ζ are,

$$\omega_\delta^2 \equiv 2\Gamma_M H, \quad \zeta \equiv (\Gamma_M + 2H)/(2\omega_\delta), \quad (3.2)$$

which weakly depends on time.

3.1 Under- and over-damped oscillating modes

We further approximately treat the slowly time-varying ω_δ and ζ as constants, compared with the rapidly time-oscillating modes Δ_M^0 and δ_M^0 under considerations. In this circumstance, the approximate solution to Eq. (3.1) reads

$$\delta_M^0 \propto e^{-\omega_\delta\zeta t} e^{-i\omega_\delta(1-\zeta^2)^{1/2}t}. \quad (3.3)$$

We have the following physical situations:

- (i) in the underdamped case ($\zeta < 1$), i.e., $2\omega_\delta > \Gamma_M + 2H$, the modes δ_M^0 and Δ_M^0 oscillate with smaller frequencies than ω_δ , their wavelengths are smaller than the horizon size, and amplitudes damped to zero inside the horizon. The damping time scale $(\omega_\delta\zeta)^{-1} = (\Gamma_M + H)^{-1} \approx \Gamma_M^{-1}$;

- (ii) in the overdamped case ($\zeta > 1$), i.e., $2\omega_\delta < \Gamma_M + 2H$, the δ_M^0 and Δ_M^0 modes' wavelengths are larger than the horizon size, and their amplitudes exponentially decay and return to steady states without oscillating. In the case ($\zeta \gg 1$), the solution (3.3) yields $\delta_M^0, \Delta_M^0 \propto \text{const.}$, indicating the amplitudes of modes δ_M^0 and Δ_M^0 are “frozen” to constants outside the horizon.

3.2 Lowest-lying mode crossing horizon

The separatrix between two situations (i) and (ii) is defined at $\zeta = 1$. At this separatrix, the frequency ω_δ and damping ratio ζ (3.2) lead to

$$\Gamma_M = 2H, \quad (3.4)$$

and the critical ratio of horizon radius and pair oscillating wavelength

$$\frac{H^{-1}}{\omega_\delta^{-1}} = \left(\frac{2\Gamma_M}{H} \right)^{1/2} = 2. \quad (3.5)$$

Such a critical ratio represents the horizon crossing of the zero modes δ_M^0 and Δ_M^0 :

- (a) subhorizon δ_M^0 and Δ_M^0 modes are *inside* the horizon for $(H^{-1}/\omega_\delta^{-1}) > 2$;
- (b) superhorizon δ_M^0 and Δ_M^0 modes are *outside* the horizon for $(H^{-1}/\omega_\delta^{-1}) < 2$.

These results have clear physical meanings. Whether the oscillating modes is the subhorizon size or superhorizon size crucially depends on the “time-competition” (3.4) between the density perturbations ($\rho_M^\pm \Leftrightarrow \rho_M^0$) rate Γ_M and the Hubble rate H of spacetime expansion: $\Gamma_M > H$ the modes stay inside the horizon; $\Gamma_M < H$ the modes stay outside the horizon. In other words, the modes stay inside (outside) the horizon, if they oscillate faster (slower) than the spacetime expanding rate, since they have (no) enough time to keep themselves inside the horizon. Consistently, the “space-competition” (3.5) of horizon size and mode wavelength shows (a) subhorizon-sized modes and (b) superhorizon-sized modes.

The horizon crossing condition (3.5) clearly depends on the functions $H(t)$ and $\Gamma_M(t)$ in different epochs of the Universe evolution. Defining the rate $\Gamma_M^{\text{cr}} = \chi \hat{m} \epsilon_{\text{cr}} / (4\pi)$ (1.3) at the horizon crossing, we find the horizon crossing condition $H_{\text{cr}} = \Gamma_M^{\text{cr}} / 2$ (3.4) for the zero mode

$$(H_{\text{cr}} / \chi \hat{m}) = (1/8\pi) \epsilon_{\text{cr}}, \quad (3.6)$$

where H_{cr} and ϵ_{cr} stand for the Hubble scale and ϵ -rate at the horizon crossing. The LHS is the ratio of massive pair plasma width and horizon radius, e.g., $(\lambda_m / H_{\text{cr}}^{-1})$. While the RHS is the ϵ -rate (1.4) depending on the horizon evolution.

We end this section by noting that the term $\dot{\Gamma}_M \propto \dot{\epsilon} > 0$ in Eqs. (2.14, 2.15) might not be negligible for fast time-increasing ϵ -rate in the \mathcal{P} -episode. The effective oscillating frequencies $\omega_\delta = 2H\Gamma_M + \dot{\Gamma}_M > 2H\Gamma_M$ (wavelengths ω_δ^{-1}) become larger (smaller). Therefore the critical ratio (3.5) should be larger than 2, compared with the case $\dot{\Gamma}_M = 0$.

3.3 Symmetric and asymmetric oscillating amplitudes at horizon crossing

To quantify symmetric and asymmetric oscillating amplitudes at horizon crossing, we define the root-mean-square (*rms*) density fluctuations by

$$\bar{\delta}_M \equiv \langle \delta_M(\mathbf{x}) \delta_M^\dagger(\mathbf{x}) \rangle^{1/2}, \quad \bar{\Delta}_M \equiv \langle \Delta_M(\mathbf{x}) \Delta_M^\dagger(\mathbf{x}) \rangle^{1/2} \quad (3.7)$$

where $\langle \dots \rangle = V_{\text{pair}}^{-1} \int d^3x (\dots)$ indicates the average all states over the space. The use of Fourier transformations (2.16) and (2.17) yields

$$\bar{\delta}_M^2 = \frac{1}{V_{\text{pair}}} \sum_{\mathbf{k}, \mathbf{k}'} \delta_M^{\mathbf{k}} \delta_M^{\mathbf{k}'\dagger} \delta_{\mathbf{k}, \mathbf{k}'} = \frac{1}{V_{\text{pair}}} \sum_{\mathbf{k}} |\delta_M^{\mathbf{k}}|^2 \quad (3.8)$$

and the same for $\bar{\Delta}_M^2$, where the dimensionless $\delta_{\mathbf{k}, \mathbf{k}'} = V_{\text{pair}}^{-1} \int d^3x e^{i\mathbf{x}(\mathbf{k}-\mathbf{k}')} \delta_{\mathbf{k}, \mathbf{k}'}$ is the Kronecker delta function of discrete variables \mathbf{k} and \mathbf{k}' .

3.3.1 Lowest-lying mode amplitudes at horizon crossing

Considering only contribution from the lowest-lying modes of underdamped oscillating δ_M^0 and Δ_M^0 , we approximately obtain from Eq. (3.8)

$$\bar{\delta}_M^2 \approx V_{\text{pair}}^{-1} |\delta_M^0|^2, \quad \bar{\Delta}_M^2 \approx V_{\text{pair}}^{-1} |\Delta_M^0|^2. \quad (3.9)$$

At a fixed time t , the amplitudes $|\delta_M^0|^2$ and $|\Delta_M^0|^2$ of the lowest lying state (ground state) of the underdamped harmonic oscillator (3.1) can be expressed by the characteristic length scale $1/(2\hat{m}\omega_\delta)^{1/2}$ of the oscillation,

$$|\delta_M^0|^2 \approx 1/(2\hat{m}\omega_\delta)^{3/2}, \quad |\Delta_M^0|^2 \approx 1/(2\hat{m}\omega_\Delta)^{3/2}, \quad (3.10)$$

see, e.g., Refs. [47], [48] and [49]. If the wavelength of the lowest-lying state is much smaller than the horizon radius, the ground state will evolve adiabatically, and Eq. (3.10) will continue to hold at later times. Thus we obtain the root-mean-square of density fluctuations (3.7)

$$\bar{\delta}_M^2 = \bar{\Delta}_M^2 \approx \frac{1}{4\pi(2\hat{m})^{3/2}} \frac{3H^3}{(2H\Gamma_M)^{3/2}}. \quad (3.11)$$

At the other extreme, if the wavelength of the lowest-lying state is much larger than the horizon radius, the oscillator will overdamp, and the oscillating amplitudes $\bar{\delta}_M$ and $\bar{\Delta}_M$ will remain constants in time. These constants at the horizon crossing $H_{\text{cr}} = \Gamma_M^{\text{cr}}/2$ (3.6) are

$$\bar{\delta}_M = \bar{\Delta}_M \approx \left(\frac{3}{32\pi} \right)^{1/2} \left(\frac{H_{\text{cr}}}{\hat{m}} \right)^{3/4} = \left(\frac{3}{32\pi} \right)^{1/2} \left(\frac{\chi \epsilon_{\text{cr}}}{8\pi} \right)^{3/4}, \quad (3.12)$$

whose values depend on the Hubble rate H or the ϵ -rate at the horizon crossing. The width parameter $\chi \sim \mathcal{O}(10^{-3})$ constrained by the CMS observations [44] and we approximately obtain the theoretical value $\chi \approx 1.85 \times 10^{-3}$ [50, 51] in the study of massive pair production ($m \gg H$).

3.3.2 Particle-antiparticle asymmetry due to horizon crossing

As a result, using Eqs. (2.12,2.13), we explicitly write the result (3.12) as,

$$\rho_M^+ - \rho_M^- = \bar{\delta}_M \rho_M^H, \quad (3.13)$$

$$\rho_M - \rho_M^H = \bar{\Delta}_M \rho_M^H, \quad (3.14)$$

where the right-handed sides are in the sense of *rms*. In other words, $\bar{\delta}_M \rho_M^H$ represents the spatial fluctuations in the number of particles or antiparticles (compositions) per comoving volume, and $\bar{\Delta}_M \rho_M^H$ represents the spatial fluctuations in the number of pairs per comoving volume. This result physically implies the following two consequences due to the particle-antiparticle oscillations at the horizon crossing:

- (i) In the case that the δ_M is an underdamped oscillating mode inside the horizon, its root-mean-squared (*rms*) value $\bar{\delta}_M$ vanishes, indicating all particles and antiparticles are inside the horizon, no net particle number appears with respect to the observer inside the horizon. The particle-antiparticle symmetry holds.
- (ii) In the case that the δ_M is an overdamped oscillating mode frozen outside the horizon, its root-mean-squared (*rms*) value $\bar{\delta}_M$ does not vanish. It indicates that some particles (or antiparticles) are outside the horizon. Thus net particle number appears with respect to the observer inside the horizon. The particle-antiparticle symmetry breaks. The “frozen” amplitudes of $\bar{\delta}_M$ and $\bar{\Delta}_M$ (3.12) are very small for $\hat{m} \gg H_{\text{cr}}$.

It is important to note that the total number of particles and antiparticles inside and outside the horizon preserves. In the second case (ii), the positive (negative) net number of particles and antiparticles viewed by a subhorizon observer has to be equal to the negative (positive) net number of particles and antiparticles outside the horizon. The asymmetric perturbation $\bar{\delta}_M$ at the horizon crossing describes particle and antiparticle number asymmetry.

4 Horizon crossings at reheating start and end

As discussed in the previous section, the lowest-lying mode δ_M inside the horizon represents an under-damping oscillation between particles and antiparticles and its dampened amplitude vanishes within the horizon. As a result, the averaged net number of particles is zero at the time period $t \sim H^{-1}$, and the symmetry of particle and antiparticle is preserved. Instead, the lowest-lying mode δ_M outside the horizon means that its amplitude is frozen to a constant $\delta_M = \text{const.} \neq 0$. It implies that the observer inside the horizon should observe a non-vanishing net particle number associating the horizon surface, representing the modes of constant amplitude outside the horizon. Such mode horizon crossing indicates the occurrence of particle and antiparticle asymmetry. Now we need to examine when such mode horizon crossing takes place in reheating. The same discussions apply to the pair-density perturbation mode Δ_M (2.12), which however does not violate the symmetry of particle and antiparticle.

4.1 Subhorizon crossing in preheating \mathcal{P} -episode

To identify the subhorizon crossing in preheating \mathcal{P} -episode, we examine that the modes δ_M and Δ_M are superhorizon size in the pre-inflation and inflation epochs, while they are subhorizon size in the massive pair oscillating \mathcal{M} -episode of the reheating epoch.

4.1.1 Particle-antiparticle asymmetry in pre-inflation and inflation

In the pre-inflation and inflation epoch $H > \Gamma_M$, the modes δ_M and Δ_M are outside the horizon, corresponding to the overdamped case ($\zeta > 1$). This can also be seen by the ratio of horizon radius H^{-1} and pair oscillating wave length ω_δ^{-1} (2.24),

$$\frac{H^{-1}}{\omega_\delta^{-1}} = \left(\frac{H^{-2}}{2^{-1}\Gamma_M^{-1}H^{-1}} \right)^{1/2} < \left(\frac{\Gamma_M^{-1}}{2^{-1}\Gamma_M^{-1}} \right)^{1/2} = 2^{1/2}, \quad (4.1)$$

indicating $H^{-1}/\omega_\delta^{-1} < 2$. We use the numerical results in Ref. [45] to show the ratio (4.1) in Fig. 1 (a), where the blue line $H^{-1}/\omega_\delta^{-1}$ is below the orange line 2. This implies that in the pre-inflation and inflation, the modes δ_M and Δ_M wavelengths are larger than the horizon size, their amplitudes exponentially decay and return to steady states without oscillating. It means that the modes δ_M and Δ_M are superhorizon size, and their amplitudes are “frozen” to constants outside the horizon. With respect to an observer inside the horizon, it means that $\bar{\delta}_M$ (3.13) does not vanish ($\bar{\delta}_M \neq 0$) and the particle-antiparticle asymmetry holds in the pre-inflation and inflation epoch ($a < a_{\text{end}}$).

4.1.2 Particle-antiparticle symmetry in \mathcal{M} -episode

In the \mathcal{M} -episode $H < \Gamma_M/2$, however, we find that the modes δ_M and Δ_M are inside the horizon. This is because the the ratio of horizon radius and pair oscillating wavelength is larger than 2,

$$\frac{H^{-1}}{\omega_\delta^{-1}} = \left(\frac{H^{-2}}{2^{-1}H^{-1}\Gamma_M^{-1}} \right)^{1/2} > \left(\frac{2\Gamma_M^{-1}}{2^{-1}\Gamma_M^{-1}} \right)^{1/2} = 2. \quad (4.2)$$

It means that the modes δ_M and Δ_M are subhorizon sized and underdamped oscillations, corresponding to the underdamped case ($\zeta < 1$). We use the numerical results in Ref. [45] to show the ratio (4.2) in Fig. 1 (a), where the blue line $H^{-1}/\omega_\delta^{-1}$ is above the orange line 2. Therefore, in the \mathcal{M} -episode the particle-antiparticle asymmetric mode δ_M and symmetric mode Δ_M are well inside the horizon, behaving as underdamped oscillating waves whose dampened amplitudes vanish within the horizon H^{-1} . Their root-mean-square density fluctuations (3.7) $\bar{\delta}_M = 0$ and $\bar{\Delta}_M = 0$ vanish. It means that with respect to an observer inside the horizon, the asymmetric perturbation $\bar{\delta}_M$ (3.13) vanishes ($\bar{\delta}_M = 0$) and the particle-antiparticle symmetry holds in the \mathcal{M} -episode.

The $\bar{\delta}_M = 0$ and $\bar{\Delta}_M = 0$ equivalently correspond to the averaged $\langle \delta_M \rangle = 0$ and $\langle \Delta_M \rangle = 0$ over the Hubble time scale $\tau_H \sim H^{-1}$, which is larger than the perturbation time scale τ_M (1.3). The $\langle \Delta_M \rangle = 0$ corresponds to the detailed balance of perturbations

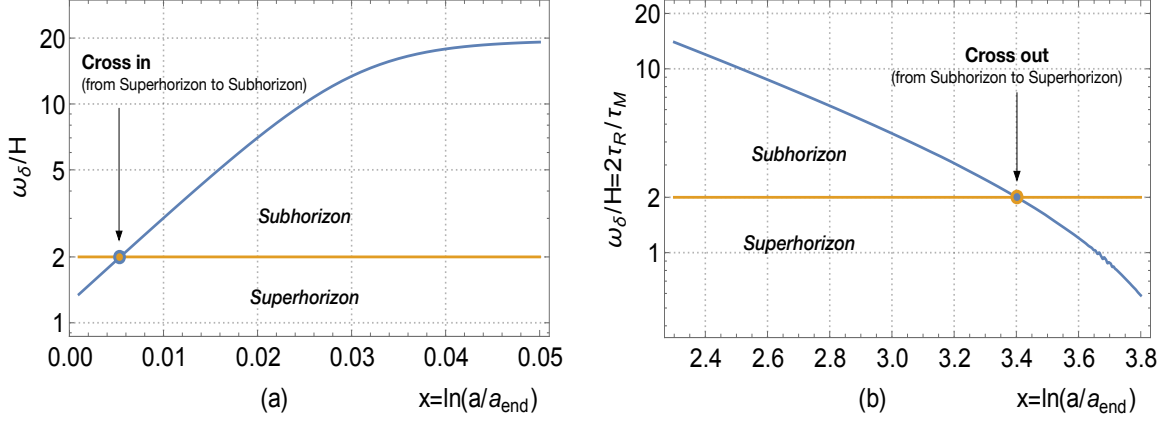


Figure 1. (Color Online). In these two figures (a) and (b), we use the previous numerical results H and Γ_M obtained by solving Eqs. (6.6-6.11) with the parameters $\hat{m}/m_{\text{pl}} = 27.7$ and $g_Y^2 = 10^{-9}$ in Ref. [45]. In terms of the e -folding number $x = \ln(a/a_{\text{end}})$, the ratio ω_δ/H (4.2) of the horizon size H^{-1} and the oscillating wavelength ω_δ^{-1} is plotted (blue), compared with the horizon crossing $\omega_\delta/H = 2$ (orange). Superhorizon (subhorizon) is below (above) the orange horizontal line. Left (a): The ratio $\omega_\delta/H = (2\Gamma_M/H)^{1/2}$ (3.5) (blue) in the preheating \mathcal{P} -episode. The modes (blue line) evolve from superhorizon to subhorizon and cross at $\ln(a_{\text{crin}}/a_{\text{end}}) \approx 0.005$ and $a_{\text{crin}} \approx 1.01 a_{\text{end}}$. Right (b): The ratio $\omega_\delta/H \approx (2\tau_R/\tau_M)$ (4.7) (blue) in the genuine reheating \mathcal{R} -episode. The modes (blue line) evolve from subhorizon to superhorizon and cross at $\ln(a_{\text{cROUT}}/a_{\text{end}}) \approx 3.4$ and $a_{\text{cROUT}} \approx 30a_{\text{end}}$. Whereas, the reheating occurs at $\ln(a_R/a_{\text{end}}) \approx 3.8$ and $a_R \approx 45 a_{\text{end}}$ from Fig. 7 (a) of Ref. [45]. Thus, $a_{\text{cROUT}} \lesssim a_R$. It shows the crossing occurs before the massive pair domination (\mathcal{M} -episode) ends. This is reason that we neglect the decay rate $\Gamma^{\text{de}} \ll \Gamma_M$ in analyzing Eq. (2.1).

$\rho_M^\pm \Leftrightarrow \rho_M^H/2$ in the rate equation (2.1). It implies the detailed balance inside the horizon. Therefore the net number of particles and antiparticles is zero and the particle-antiparticle symmetry preserves.

4.1.3 Subhorizon crossing and particle-antiparticle symmetry

From the superhorizon size (4.1) in the inflation epoch to the subhorizon size (4.2) in the \mathcal{M} -episode, the modes δ_M and Δ_M cross at least once the horizon. Because the H and Γ_M vary monotonically, Equations (4.1) and (4.2) show that one horizon crossing point $\omega_\delta = H$ locates at $H = \Gamma_M/2$ in the preheating \mathcal{P} -episode. Using Eq. (3.4), we find the subhorizon crossing scale H_{crin} and the oscillating frequency $\omega_\delta^{\text{crin}}$ at the scale factor a_{crin} ,

$$H_{\text{crin}} = \Gamma_M/2 \approx H_{\text{end}}/2, \quad \omega_\delta^{\text{crin}} = (2\Gamma_M H)^{1/2} \approx H_{\text{end}}, \quad (4.3)$$

which are the same order of the inflation end scale $H_{\text{end}} \approx \Gamma_M$. In Fig. 1 (a), using previous numerical results, we plot the ratio $H^{-1}/\omega_\delta^{-1} = (2\Gamma_M/H)^{1/2}$ (4.2), starting from the inflation end H_{end} , to show the subhorizon crossing takes place at $x = \ln(a_{\text{crin}}/a_{\text{end}}) \approx 5 \times 10^{-3}$, i.e., $a_{\text{crin}} \approx 1.01a_{\text{end}}$ in the preheating \mathcal{P} -episode. It shows that the subhorizon crossing occurs right after the inflation end, $H_{\text{crin}} > H_{\text{end}}$ and $a_{\text{crin}} \gtrsim a_{\text{end}}$.

In the pre-inflation and inflation epoch, the subhorizon observer views the particle-antiparticle asymmetry because some of the particles or antiparticles are outside the horizon. When these superhorizon particles or antiparticles cross back the horizon, the subhorizon observer views all particles and antiparticles, therefore the particle-antiparticle symmetry. The number of particles or antiparticles subhorizon crossing at a_{crin} can be calculated as follow. The numerical value $\epsilon_{\text{cr}} = \epsilon_{\text{crin}} \approx 1.0 \times 10^{-2}$ at the subhorizon crossing a_{crin} can be found from the Figure 6 (c) of Ref. [45]. We use Eq. (3.12) to calculate the asymmetric and symmetric pair density perturbations

$$\bar{\delta}_M^{\text{crin}} = \bar{\Delta}_M^{\text{crin}} \approx 4.33 \times 10^{-6}, \quad (4.4)$$

at the subhorizon crossing. Then the net particle density perturbation (3.13) and the pair density perturbation (3.14) at the subhorizon crossing (4.3) are given by,

$$\rho_M^+ - \rho_M^- = \bar{\delta}_M^{\text{crin}} \rho_M^H \approx \bar{\delta}_M^{\text{crin}} (\hat{m}^2 H_{\text{end}}^2)/2, \quad (4.5)$$

$$\rho_M - \rho_M^H = \bar{\Delta}_M^{\text{crin}} \rho_M^H \approx \bar{\Delta}_M^{\text{crin}} (\hat{m}^2 H_{\text{end}}^2)/2. \quad (4.6)$$

They are about 10^{-3} in unit of the characteristic density $\rho_{\text{end}}^c = 3m_{\text{pl}}H_{\text{end}}^2$ in the preheating \mathcal{P} -episode. The particle-antiparticle asymmetry (4.5) is on the horizon surface at the subhorizon crossing. It represents the superhorizon particle-antiparticle asymmetry in the pre-inflation and inflation epochs. It also represents the subhorizon restoration of the practice-antiparticle symmetry in the \mathcal{M} -episode.

After the subhorizon crossing (4.3), the subhorizon sized modes δ_M and Δ_M remain inside the horizon as underdamped oscillating modes in the \mathcal{M} -episode, as shown in Fig. 1 (a), until they undergo the superhorizon crossing again.

4.2 Superhorizon crossing in genuine reheating \mathcal{R} -episode

We will show the modes δ_M and Δ_M superhorizon crossing in the transition period from the massive pair \mathcal{M} -episode to the genuine reheating \mathcal{R} -episode. Unstable massive pairs predominately decay into light particles in the Standard Model (SM) of particle physics in the \mathcal{R} -episode.

4.2.1 Superhorizon crossing in reheating

In the genuine reheating \mathcal{R} -episode, the horizon scale H is mainly determined by unstable pairs' decay since the pair decay rate Γ_M^{de} (time τ_R) is much larger (shorter) than the rate Γ_M (time τ_M) of massive pair perturbations. To see the modes δ_M and Δ_M are subhorizon size or superhorizon size in the \mathcal{R} -episode, we use the criteria (3.4) or (3.5),

$$\frac{H^{-1}}{\omega_\delta^{-1}} = \left(\frac{2\Gamma_M}{H} \right)^{1/2} \approx 2(\tau_R \Gamma_M)^{1/2} = 2 \left(\frac{\Gamma_M}{\Gamma_M^{\text{de}}} \right)^{1/2} < 2. \quad (4.7)$$

Here we adopt the horizon size H^{-1} approximately determined by the reheating scale H_{RH} at the scale factor a_R , see Eq. (7.31) of Ref. [45] or the first equation in (5.74) of Ref. [46],

$$H_{\text{RH}}^2 = (2\tau_R)^{-2} = (\Gamma_M^{\text{de}}/2)^2, \quad (4.8)$$

and $\Gamma_M^{\text{de}} > \Gamma_M$ in the \mathcal{R} -episode. The inequality (4.7) or $\Gamma_M < 2H_{\text{RH}} \approx \Gamma_M^{\text{de}}$ [see Eq. (3.4)] shows that the modes δ_M and Δ_M are superhorizon sizes in the \mathcal{R} -episode.

From the subhorizon-sized modes in the \mathcal{M} -episode to the superhorizon-sized modes in the \mathcal{R} -episode, the δ_M and Δ_M modes' superhorizon crossing must take place in the transition period between the \mathcal{M} -episode and the \mathcal{R} -episode. The superhorizon crossing occurs at $H^{-1}/\omega_\delta^{-1} = 2$, yielding

$$H_{\text{crou}} = \Gamma_M^{\text{crou}}/2 \approx \Gamma_M^{\text{de}}/2, \quad \Gamma_M^{\text{crou}} \approx \Gamma_M^{\text{de}}, \quad (4.9)$$

consistently with the horizon crossing condition (3.4) or (3.5). The approximation $\Gamma_M^{\text{crou}} \approx \Gamma_M^{\text{de}}$ comes from $H_{\text{crou}} \approx H_{\text{RH}} = (\Gamma_M^{\text{de}}/2)$. It implies that the superhorizon crossing occurs at

$$H_{\text{crou}} \gtrsim H_{\text{RH}}, \quad a_{\text{crou}} \lesssim a_R, \quad (4.10)$$

near to the reheating scale H_{RH} and a_R .

To verify such a superhorizon crossing point (4.9), we use previous numerical results to plot the ratio $H^{-1}/\omega_\delta^{-1} \approx 2\tau_R/\tau_M$ of the horizon radius and pair density perturbation wavelength in Fig. 1 (b). It shows that the ratio $H^{-1}/\omega_\delta^{-1}$ (blue line) varies from subhorizon (> 2) to superhorizon (< 2). The superhorizon crossing H_{crou} and a_{crou} (4.10) are indeed close to the genuine reheating H_{RH} and a_R (4.8), determined by $\tau_R \approx \tau_D$ in the Fig. 7 (c) and (d) of Ref. [45].

4.2.2 Initial particle-antiparticle asymmetry for standard cosmology

As illustrated in Figs. 1 (a) and (b), the modes δ_M and Δ_M have the subhorizon crossing (4.3) in the preheating \mathcal{P} -episode and superhorizon crossing (4.10) in the genuine reheating \mathcal{R} -episode. The subhorizon observer views:

- (i) the particle and antiparticle asymmetry in the pre-inflation and inflation epochs before the subhorizon crossing (4.3), and the asymmetry is given by Eq. (4.5);
- (ii) the particle and antiparticle symmetry in the massive pair \mathcal{M} -episode between the preheating and genuine reheating episodes;
- (iii) the initial particle and antiparticle asymmetry in standard cosmology after the genuine reheating \mathcal{R} -episode.

We have discussed (i) and (ii), and will focus on (iii) and calculate the initial particle and antiparticle asymmetry for the standard cosmology. Due to the superhorizon crossing $a_{\text{crou}} \lesssim a_R$, the δ_M is an overdamped oscillating mode frozen outside the horizon, its root-mean-squared (*rms*) value $\bar{\delta}_M$ does not vanish. It indicates that some particles (or anti-particles) are outside the horizon, thus net particle number appears, viewed by the subhorizon observer, in the standard cosmology.

Using Eq. (3.12), we obtain the asymmetric and symmetric pair density perturbations at the superhorizon crossing (4.9)

$$\bar{\delta}_M^{\text{crou}} = \bar{\Delta}_M^{\text{crou}} = 2.31 \times 10^{-4}, \quad (4.11)$$

by using $\epsilon_{\text{cr}} = \epsilon_{\text{crou}} \approx 2$ closes to the genuine reheating \mathcal{R} -episode. Based on Eq. (3.13), we calculate the particle-antiparticle asymmetric number density, i.e., the net number density of particles and antiparticles,

$$\delta n_M^{\text{crou}} = \frac{\rho_M^+ - \rho_M^-}{2\hat{m}} = \bar{\delta}_M^{\text{crou}} n_M^H|_{\text{crou}}, \quad (4.12)$$

at the superhorizon crossing $H_{\text{crou}} \gtrsim H_{\text{RH}}$ and $a_{\text{crou}} \lesssim a_R$. As a result, we approximately obtain the net number density of massive particles and antiparticles,

$$\delta n_M^{\text{crou}} = \frac{\rho_M^+ - \rho_M^-}{2\hat{m}} \Big|_{\text{crou}} \approx 2.31 \times 10^{-4} n_M^H|_{\text{crou}}, \quad (4.13)$$

and $n_M^H|_{\text{crou}} \approx \chi \hat{m} H_{\text{RH}}^2$. Analogously, we obtain from Eq. (3.14) the pair number density perturbation of massive particles,

$$\Delta n_M^{\text{crou}} = \frac{\rho_M - \rho_M^H}{2\hat{m}} \Big|_{\text{crou}} \approx 2.31 \times 10^{-4} n_M^H|_{\text{crou}}. \quad (4.14)$$

This net number density (4.13) of massive particles and antiparticles is the initial value of the asymmetric (net) numbers of particles and antiparticles in the standard cosmology.

After the superhorizon crossing (4.10) in reheating, unstable massive pairs rapidly decay to light particles for $\tau_R \ll \tau_M$ and $\Gamma_M^{\text{de}} \rho_M^\pm$ domination (2.1), and the density perturbations $\rho_M^\pm \Leftrightarrow \rho_M^0$ is no longer relevant for unstable pairs. The asymmetric modes δ_M carried the net particle number has been frozen in the superhorizon. Such a nonzero net number of particles and antiparticles inside the horizon preserves during the entire history of the standard cosmology. To illustrate our discussions, in Fig. 2 we schematically show the particle-antiparticle pair symmetry and asymmetry epochs, and indicate the occurrences of subhorizon cross in and superhorizon cross out.

It is important to note that the total number of particles and antiparticles inside and outside the horizon is zero and preserved. The positive (negative) net number of particles and antiparticles viewed by a subhorizon observer has to be equal to the negative (positive) net number of particles and antiparticles outside the horizon. The latter is described by the asymmetric perturbation $\bar{\delta}_M$ on the surface of the superhorizon crossing. The sum of these two net numbers is identically zero, because the particle and antiparticle symmetry is preserved in the $\rho_M^\pm \Leftrightarrow \rho_M^0$ processes, pair decay process $\bar{F}F \Rightarrow \bar{\ell}\ell$ and all other microscopic processes respect the CPT symmetry.

5 Baryogenesis and magnetogenesis in reheating epoch

A tiny asymmetry (net number) of particles and antiparticles remains inside the horizon and the subhorizon observer views a nonzero net number of particles and antiparticles. We will show that the asymmetry of massive particles F and antiparticles \bar{F} results in the asymmetry of baryon numbers of baryons B and antibaryons \bar{B} in the Universe, and the net number density (4.13) leads to baryogenesis in agreement with observations.

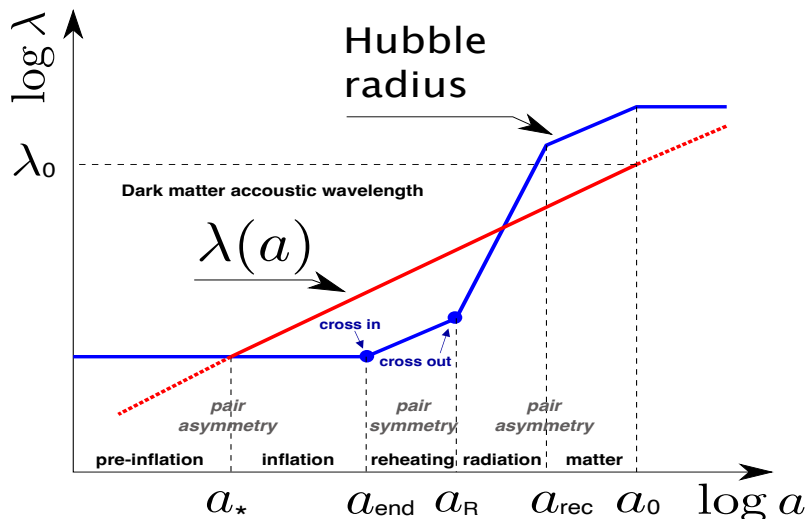


Figure 2. We make this figure by modifying Fig. 1 in Ref. [52] to illustrate schematic evolution of the Hubble radius H^{-1} and the physical wavelength $\lambda(a)$ of dark matter acoustic wave. The wavelength $\lambda_0 = \lambda(a_0)$ at the present time $a_0 = 1$ crossed the Hubble horizon H_* at the early time a_* , fixed by the physically interesting length scale $\lambda_0 = \lambda_* = k_*^{-1}$. The pre-inflation $a > a_*$, the inflation $a_* < a < a_{\text{end}}$, the reheating $a_{\text{end}} < a < a_R$, and the recombination at a_{rec} . The horizon “cross in” point corresponds to the point in Fig. 1 (a). The horizon “cross out” point corresponds to the point in Fig. 1 (b). The reheating epoch holds particle and antiparticle pair symmetry. The pre-inflation, inflation, radiation, and matter epochs do not hold particle and antiparticle pair symmetry.

5.1 Origin of net baryon numbers

Following the approach discussed in Ref. [46], we use the net particle number density $\delta n_M^{\text{crou}}t$ (4.13) and the continuity equation of the net baryon number density n_B to obtain

$$\begin{aligned} \dot{n}_B + 3Hn_B &= \delta n_M^{\text{crou}}t / \tau_R, \\ \Rightarrow n_B(a) &= 2.31 \times 10^{-4} n_M^H(a_R) \left(\frac{a}{a_R} \right)^{-3} [1 - \exp -t/\tau_R]. \end{aligned} \quad (5.1)$$

In the second line of integration, the initial moment $t_i \ll \tau_R$ is assumed and the solution for massive pairs ρ_M decay is used, see Eq. (7.23) of Ref. [45] or the first equation in (6.61) of Ref. [46]. The physical content is clear: at late times, $t \gg \tau_R$, the net baryon number per comoving volume $a^3 n_B(a)$ is just 2.31×10^{-4} times the initial number of massive particles per comoving volume $a_R^3 n_M^H(a_R)$. Note that $a^3 n_B(a)$ is the comoving number density, whereas $n_B(a)$ is the physical number density, i.e., the net baryon number per physical volume. Since the decay time scale $\tau_R \propto \hat{m}^{-1}$ is very short, we adopt the approximation that the horizon crossing coincides with the genuine reheating (4.10) ($a = a_R \approx a_{\text{crou}}t$ and $t \approx \tau_R$) to obtain the net baryon number density

$$n_B^R(a_R) = 1.46 \times 10^{-4} n_M^H(a_R), \quad n_M^H(a_R) = \chi \hat{m} H_{\text{RH}}^2. \quad (5.2)$$

It yields the origin of the net number of baryons or antibaryons, i.e., the baryogenesis in the Universe.

As an asymmetric relic from the reheating epoch or as an initial asymmetric state of the standard cosmology, the net baryon number (5.2) remains inside the horizon and conserves in subsequent Universe evolution. It accounts for the baryon and anti-baryon asymmetry observed today. It should be emphasized that in our scenario the standard cosmology starts from the initial state of asymmetrical baryon and antibaryon numbers. Therefore the three Sakharov criteria [53] for the baryogenesis are not applicable.

5.2 Baryon number-to-entropy ratio

Using the entropy S_R and temperature T_{RH} of the reheating epoch, obtained in Eqs. (8.6) and (8.8) of Ref. [45], we calculate the baryon asymmetry represented by the ratio of the net baryon number $a_R^3 n_B^R$ (5.2) to the entropy S_R . Per comoving volume, this ratio at the reheating a_R is given by

$$\frac{n_B^R}{s_R} = \frac{a_R^3 n_B^R}{S_R} \approx 1.46 \times 10^{-4} \frac{a_R^3 n_M^H(a_R)}{S_R} \approx 2.6 \times 10^{-4} \frac{T_{RH}}{\hat{m}}, \quad (5.3)$$

where the entropy density $s_R = S_R/a_R^3$ at the genuine reheating \mathcal{R} -episode. This result is consistent with the one derived from the processes of baryon-number violating decay in Ref. [46]. This baryon number-to-entropy ratio n_B^R/s_R (5.3) preserves its value from the reheating epoch to the present time. The present observational value is $n_B/s = 0.864_{-0.015}^{+0.016} \times 10^{-10}$ [18]. This determines the ratio of the reheating temperature T_{RH} to the mass parameter \hat{m} ,

$$(T_{RH}/\hat{m}) \approx 3.3 \times 10^{-7}. \quad (5.4)$$

It is used to constrain the parameters $(g_Y^2/g_*^{1/2})$ and (\hat{m}/M_{pl}) , see Eq. (8.11) of Ref. [45], g_* is the effective degeneracy of SM light particles $\ell\bar{\ell}$ produced in reheating.

5.3 Magnetogenesis via baryogenesis

We show how magnetogenesis achieves via the baryogenesis in this scenario. Suppose that the Universe is spatially homogeneous at the moment a_R of baryogenesis and reheating (4.10). The net particle number density $\delta n_M^{\text{crou}}t$ (4.13) is generated, consequently resulting in the net baryon number density n_B^R (5.2). These net baryons carry electric charges and their density n_B^R can generate an electric current density

$$\vec{j}_B \approx e \vec{v}_B n_B^R, \quad (5.5)$$

where e is the absolute value of electron charge and the velocity \vec{v}_B represents the spacetime-averaged relative velocity

$$\vec{v}_B \equiv \langle \delta \mathbf{v}_M \rangle = \langle \mathbf{v}_M^+ - \mathbf{v}_M^- \rangle / 2, \quad v_B \equiv |\langle \delta \mathbf{v}_M \rangle| \quad (5.6)$$

between the velocities of positively and negatively charged particles, see Eq. (2.5). Provided the non-vanishing relative velocity $|\vec{v}_B| \neq 0$ and electric current density $|\vec{j}_B| \neq$

0, a nontrivial primordial magnetic field B_R must be generated and frozen inside the horizon. It associating to the net baryon number density n_B^R (5.2).

Denote that inside the horizon at the reheating, B_R represents the primordial magnetic field in the coordinate frame. To estimate the upper and lower limits of the primordial magnetic field B_R , we use the integral form of the Maxwell equation,

$$\oint_{\ell_R} \vec{B}_R \cdot d\vec{\ell} = 4\pi \oint_{\mathcal{A}_R} \vec{j}_B \cdot d\vec{\sigma}, \quad (5.7)$$

where the area $\mathcal{A}_R = \pi H_{\text{RH}}^{-2}$ and its boundary $\ell_R = 2\pi H_{\text{RH}}^{-1}$ inside the horizon.

5.3.1 Upper limit of primordial magnetic fields

To estimate the upper limit of primordial magnetic fields, we assume an extreme circumstance that the pair relative velocity $\delta\mathbf{v}_M$ directions “orderly” distribute and the averaged relative velocity v_B (5.6) is about the speed of light. It gives the upper limit of the primordial magnetic field B_R at the reheating,

$$B_R(2\pi)H_{\text{RH}}^{-1} < \pi H_{\text{RH}}^{-2}(4\pi e)n_B^R(a_R). \quad (5.8)$$

As a result, by using the net baryon number density n_B^R (5.2), we obtain in the unit of the critical field value $B_c = m_e^2/e \approx 4 \times 10^{14}$ Gauss

$$\begin{aligned} \frac{B_R}{B_c} &< \frac{2\pi\alpha}{m_e^2 H_{\text{RH}}} 1.46 \times 10^{-4} n_B^R(a_R) \\ &\approx 1.46 \times 10^{-4} (2\pi\alpha\chi) \frac{\hat{m} H_{\text{RH}}^2}{m_e^2 H_{\text{RH}}}, \end{aligned} \quad (5.9)$$

where m_e is the electron mass and α is the fine structure constant. Further adopting the reheating scale H_{RH} (4.8) and the relation (T_{RH}/\hat{m}) (5.4), we obtain the upper limit of the primordial magnetic field at the reheating

$$\frac{B_R}{B_c} < 3.89 \times 10^{-7} \left(\frac{8\pi g_*}{90}\right)^{1/2} \left(\frac{\hat{m}}{m_e}\right)^2 \left(\frac{\hat{m}}{M_{\text{pl}}}\right) \left(\frac{T_{\text{RH}}}{\hat{m}}\right)^2 \quad (5.10)$$

$$B_R < 3.4 \times 10^{40} \left(\frac{g_*}{90}\right)^{1/2} \left(\frac{\hat{m}}{M_{\text{pl}}}\right)^3 \text{ Gauss}. \quad (5.11)$$

This result depends on the ratio (\hat{m}/M_{pl}) that is a function of the tensor-to-scalar ratio r , see Fig. 10 (left) of Ref. [45].

By the total magnetic flux conservation from the Maxwell Equation $\vec{\nabla} \cdot \vec{B} = 0$, the primordial magnetic field reduces to its present value $B_0 = (a_R/a_0)^2 B_R$ [40,41]. As a result, we obtain the upper limit of the primordial magnetic field observed today,

$$B_0 = (a_R/a_0)^2 B_R < 3.4 \times 10^{-14} \left(\frac{g_*}{90}\right)^{1/2} \left(\frac{\hat{m}}{M_{\text{pl}}}\right)^3 \text{ Gauss} \quad (5.12)$$

where $a_0/a_R = (g_*/2)^{1/3}(T_{\text{TH}}/T_{\text{CBM}})$, see Eq. (8.4) of Ref. [45]. Using the reheating $T_{\text{RH}} \sim 10^{15}$ GeV, the radiation-matter equilibrium temperature $T_{\text{eq}} \sim 10$ eV and

the entropy conservation $T_{\text{RH}} a_R \approx T_{\text{eq}} a_{\text{eq}}$, we estimate $(a_R/a_0) = (a_R/a_{\text{eq}})(a_{\text{eq}}/a_0) \sim 10^{-23} \times 10^{-4} \sim 10^{-27}$, where a_{eq} and a_0 are the scale factors at the radiation-matter equilibrium and the present time. Considering $g_* \sim 10^2$ for the SM particle physics and $(\hat{m}/M_{\text{pl}}) \approx 4$ for $r \approx 0.044$ in Fig. 10 (left) of Ref. [45], we obtain $B_0 < 4.48 \times 10^{-12} \text{G}$, consistently with the observed upper limit $B_{1\text{Mpc}} < 10^{-9} \text{G}$ [36]. On the other hand, the observed upper limit $B_{1\text{Mpc}} < 10^{-9} \text{G}$ implies the ratio $(\hat{m}/M_{\text{pl}}) < 100$. It indicates the tensor-to-scalar ratio $r < 0.0458$ from Fig. 10 (left) of Ref. [45].

5.3.2 Lower limit of primordial magnetic fields

Another extreme situation is that in the reheating epoch, the directions and values of relative velocities $\delta \mathbf{v}_M$ of positively and negatively charged particles “randomly” distribute. The averaged relative velocity $v_B = |\vec{v}_B| = 0$ and the electric current density $|\vec{j}_B| = 0$ identically vanish in Eqs. (5.5) and (5.6). Therefore the primordial magnetic field B_R is equal to zero. It could be the case if all oscillating modes of positively and negatively charged particles were subhorizon size, i.e., no horizon crossing could occur. However, the relative velocity (5.6) should not vanish $|\vec{v}_B| \neq 0$ for the occurrence of horizon crossing of particle-antiparticle oscillating modes. The reason for $|\vec{v}_B| \neq 0$ is similar to that for the non-vanishing asymmetric density perturbation $\bar{\delta}_M^{\text{crou}} \neq 0$ (4.12) at the horizon crossing, as discussed in Sec. 4.2.

We can approximately calculate the minimal value of the relative velocity $|\vec{v}_B| \neq 0$ from Eqs. (2.9) and (5.6), yielding

$$\begin{aligned} \nabla \cdot \delta \mathbf{v}_M &= -(\dot{\delta}_M^+ - \dot{\delta}_M^-) - \Gamma_M(\delta_M^+ - \delta_M^-) \\ &= -d\bar{\delta}_M/dt - \Gamma_M \bar{\delta}_M = -\Gamma_M \bar{\delta}_M. \end{aligned} \quad (5.13)$$

The second line is evaluated on the horizon where the mode amplitude $\bar{\delta}_M$ (3.12) is frozen as a constant and $d\bar{\delta}_M/dt = 0$. By using the Gauss law for the spherically symmetric case, we find the minimal value approximately

$$|\delta \mathbf{v}_M|_{\text{min}} = \frac{4\pi H^{-3} \Gamma_M \bar{\delta}_M^{\text{crou}}}{3 \cdot 4\pi H^{-2}} = \frac{\Gamma_M \bar{\delta}_M^{\text{crou}}}{3H} \approx \frac{2}{3} \bar{\delta}_M^{\text{crou}}, \quad (5.14)$$

and $\bar{\delta}_M^{\text{crou}} = 2.31 \times 10^{-4}$ (4.11), evaluated at the superhorizon crossing $H_{\text{crou}} = \Gamma_M^{\text{crou}}/2$ (4.9). The minimal value $|\delta \mathbf{v}_M|_{\text{min}}$ (5.14) gives rise to the lower limit of primordial magnetic fields generated at reheating.

Following the same calculations for the upper limit and replacing $|\vec{v}_B| = 1$ by $|\vec{v}_B| = |\delta \mathbf{v}_M|_{\text{min}}$, we obtain the lower limit of primordial magnetic fields generated at reheating

$$B_R > 5.24 \times 10^{36} \left(\frac{g_*}{90}\right)^{1/2} \left(\frac{\hat{m}}{M_{\text{pl}}}\right)^3 \text{ Gauss}, \quad (5.15)$$

and its corresponding value at present,

$$B_0 = (a_R/a_0)^2 B_R > 5.24 \times 10^{-18} \left(\frac{g_*}{90}\right)^{1/2} \left(\frac{\hat{m}}{M_{\text{pl}}}\right)^3 \text{ Gauss}. \quad (5.16)$$

Using the same range of parameters for the upper limit case: $g_* \sim 10^2$ and $(\hat{m}/M_{\text{pl}}) \approx 4$ for $r \approx 0.044$ in Fig. 10 (left) of Ref. [45], we obtain $B_0 > 6.9 \times 10^{-16} \text{G}$, consistently with the observed lower limit $B_{(>1\text{Mpc})} > 10^{-17} \text{G}$ [35].

As a result, we obtain the theoretical lower and upper limits of primordial magnetic fields generated at the reheating epoch and observed at the present time

$$4.48 \times 10^{-12} > B_0 > 6.9 \times 10^{-16} \quad \text{Gauss.} \quad (5.17)$$

These are approximate results since they depend on the scale factor $(a_R/a_0)^2$, the effective degeneracy g_* of SM light particles and the mass parameter (\hat{m}/M_{pl}) of massive pair plasma state. However, we are certain that the primordial magnetic field has upper and lower limits in this theoretical scenario.

6 Dark-matter acoustic wave and large-scale structure

We describe in Sec. 2 the density perturbations $\delta_M^{\mathbf{k}}$ and $\Delta_M^{\mathbf{k}}$ of massive particle-antiparticle pair plasma. We focus on the “zero mode” $|\mathbf{k}| = 0$ oscillations δ_M^0 and Δ_M^0 of the frequency $\omega = (2H\Gamma)^{1/2}$ in Sec. 3. We study their horizon crossings in Sec. 4, that account for the baryogenesis and magnetogenesis in Sec. 5. Note that these “zero modes” $|\mathbf{k}| = 0$ are oscillating modes, differing from wave-propagating modes $|\mathbf{k}| \neq 0$ discussed below.

From this section, we will study wave-propagating modes $\delta_M^{\mathbf{k}}$ and $\Delta_M^{\mathbf{k}}$ ($|\mathbf{k}| \neq 0$) of the frequencies $\omega_{\delta, \Delta}(|\mathbf{k}|)$ (2.20) and (2.21). They represent dark-matter acoustic waves, as indicated by the red line in Fig. 2, that exited from (superhorizon crossing out) the horizon and reentered into (subhorizon crossing in) the horizon again. In particular, we focus on the pair symmetric density perturbation modes $\Delta_M^{\mathbf{k}}$. We examine the negative term $4\pi G\rho_M^H \Delta_M^{\mathbf{k}}$ in the frequency $\omega_{\Delta}(|\mathbf{k}|)$ (2.21) to study the Jeans instability for the cases: (a) the pre-inflationary epoch where the mass parameter $m \gtrsim H$ and $v_s^2 \lesssim 1$, namely, pairs can be relativistic; (b) the inflationary epoch where the mass parameter $m \gg H$ and $v_s^2 \ll 1$, namely pairs are non-relativistic. To be specific, we turn to investigate the wave-propagating modes $\Delta_M^{\mathbf{k}}$ and $\delta_M^{\mathbf{k}}$ ($|\mathbf{k}| \neq 0$) to understand:

- (i) their superhorizon crossings out in the pre-inflation and inflation epochs, and frozen or amplified outside of the horizon;
- (ii) their subhorizon crossings in after the recombination, yielding peculiar “dark-matter” acoustic waves imprinting on the matter power spectrum at large length scales;
- (iii) their possible impacts on the formation of large-scale structures and galaxy profiles.

To start with, we would like to emphasize that the perturbations discussed here are the kinds of acoustic waves of the dispersion relations (2.20) and (2.21). They are due to fluctuations in the form of the local equation of the state $\omega_M = v_s^2$ (2.11) of particles and antiparticles, namely, spatial fluctuations in the number of particles

or antiparticles (compositions) per comoving volume. It differs from the curvature perturbations as fluctuations in energy density characterized by the local value of the spatial curvature of the spacetime.

6.1 Pair-density and particle-antiparticle-density perturbations

The wave modes are described by the comoving momentum $|\mathbf{k}|$ (wavelength $\lambda = |\mathbf{k}|^{-1}$), whose value is constant in time. As a reference, we consider the pivot scale $k^* = 0.05(\text{Mpc})^{-1}$, at which the curvature perturbations cross outside and inside horizons twice, accounting for the CMB observations. The corresponding values of the horizon $k^* = (Ha)_*$, the ϵ -rate $\epsilon = \epsilon^*$ and the mass parameter $m = m_*$ for inflation, that are given in Sec. 6 of Ref. [44] or [45].

The case $|\mathbf{k}| > k^*$ corresponds to the wave modes that exit the horizon in the pre-inflation epoch and reenter the horizon after the recombination epoch. The case $|\mathbf{k}| < k^*$ corresponds to the wave modes that exit the horizon in the inflation epoch and reenter the horizon before the recombination epoch. In both cases, $H \gg \Gamma_M = (\chi/4\pi)m\epsilon$ and $\epsilon \ll 1$. Wave equations (2.18) and (2.19) approximately become,

$$\ddot{\delta}_M^{\mathbf{k}} + 2H\dot{\delta}_M^{\mathbf{k}} \approx -\omega_\delta^2(|\mathbf{k}|)\delta_M^{\mathbf{k}}, \quad (6.1)$$

$$\ddot{\Delta}_M^{\mathbf{k}} + 2H\dot{\Delta}_M^{\mathbf{k}} \approx -\omega_\Delta^2(|\mathbf{k}|)\Delta_M^{\mathbf{k}}, \quad (6.2)$$

where the Hubble rate H slowly varies $H \approx \text{const}$. Following the same discussions in previous Sec. 3 or the usual discussions of the curvature perturbations, these wave modes $\delta_M^{\mathbf{k}}$ and $\Delta_M^{\mathbf{k}}$ of $|\mathbf{k}| \neq 0$ cross horizon from the subhorizon to the superhorizon when $\omega_{\delta,\Delta}(|\mathbf{k}|) = 2H$ (3.5), see Fig. 2. We use the frequencies $\omega_{\delta,\Delta}(|\mathbf{k}|)$ (2.20) and (2.21) to obtain the wavenumber $|\mathbf{k}|_{\delta,\Delta}$ at the superhorizon crossing,

$$|\mathbf{k}|_{\delta\text{cross}}^2 = \left(4 - \chi \frac{\epsilon m}{2\pi H}\right) \frac{(Ha)^2}{v_s^2} \Big|_{\text{cross}} \approx 4 \frac{(Ha)^2}{v_s^2} \Big|_{\text{cross}}, \quad (6.3)$$

$$\begin{aligned} |\mathbf{k}|_{\Delta\text{cross}}^2 &= \left[4 - \chi \frac{\epsilon m}{2\pi H} + \chi \left(\frac{m}{m_{\text{pl}}}\right)^2\right] \frac{(Ha)^2}{v_s^2} \Big|_{\text{cross}} \\ &\approx 4 \frac{(Ha)^2}{v_s^2} \Big|_{\text{cross}} \approx |\mathbf{k}|_{\delta\text{cross}}^2. \end{aligned} \quad (6.4)$$

These horizon-crossing conditions are for both the pre-inflation $H \lesssim m$ and the inflation $H \ll m$. They depend on the sound velocity v_s value (2.11), which decreases from the relativistic case $v_s \lesssim 1$ (pre-inflation $m \gtrsim H$) to the non-relativistic case $v_s \ll 1$ (inflation $m \gg H$). It is due to the horizon H decreases and the equation of state $p_M^H = \omega_M^H \rho_M^H$ (1.2) changes from $\omega_M^H \lesssim 1/3$ to $\omega_M^H \approx 0$ [44, 51].

The horizon crossing (6.3) and (6.4) show that because of $v_s^2 < 1$, the modes $|\mathbf{k}|_{\delta\text{cross},\Delta\text{cross}} > k^*$ cross the horizon before the inflation start $k^* = (Ha)_*$, and reenter the horizon after the recombination $(Ha)_*$. Therefore, these acoustic wave perturbations can not cross outside the horizon in the inflation epoch, then cross inside the horizon before recombination. Whereas the acoustic wave perturbations can cross to outside the horizon in the pre-inflation epoch and then cross inside the horizon after

the recombination. Therefore, the acoustic wave modes of larger $|\mathbf{k}|_{\delta_{\text{cross}, \Delta_{\text{cross}}}}$ exit the horizon earlier and reenter the horizon later and they should leave their imprints on the linear regime of large-scale structure and the nonlinear regime of galaxy clustering. We called these acoustic wave modes “dark-matter” waves [44, 51], and will discuss them in some detail below.

6.2 Pair-density perturbation and large-scale structure

The particle-antiparticle symmetric modes $\Delta_M^{\mathbf{k}}$ (2.13) represent the acoustic waves of pair-density perturbations of the dispersion relation (2.21). It is analogous to the matter density perturbation wave in gravitation fields. We examine the dispersion relation (2.21) to check whether the Jeans instability occurs and the $\Delta_M^{\mathbf{k}}$ amplitudes amplify for imaginary frequencies $\omega_\Delta^2(|\mathbf{k}|) < 0$, i.e.,

$$|\mathbf{k}|_\Delta^2 < |\mathbf{k}|_{\text{Jeans}}^2 \equiv \chi \left[\left(\frac{m}{m_{\text{pl}}} \right)^2 - \frac{\epsilon m}{2\pi H} \right] \frac{(Ha)^2}{v_s^2}. \quad (6.5)$$

The $\omega_\Delta^2(|\mathbf{k}|) = 0$ gives the Jeans wavenumber $|\mathbf{k}|_{\text{Jeans}}$ and wavelength $\lambda_{\text{Jeans}} = |\mathbf{k}|_{\text{Jeans}}^{-1}$. The modes $\Delta_M^{\mathbf{k}}$ of wavelengths $\lambda > \lambda_{\text{Jeans}}$ undergo the Jeans instability, due to the gravitational attraction of pair-density perturbations prevails.

In the inflation epoch, the gravitational attractive term $4\pi G\rho_M^H$ is negligible compared with the term $2H\Gamma_M$ in the frequency ω_Δ^2 (2.21). Thus $\omega_\Delta^2 > 0$ and the Jeans instability does not occur. In the pre-inflation epoch, instead, the term $2H\Gamma_M$ is negligible compared with the gravitational attractive term $4\pi G\rho_M^H$. It is then possible to have the imaginary frequency (2.20) $\omega_\Delta^2 < 0$ for $|\mathbf{k}|_\Delta^2 < |\mathbf{k}|_{\text{Jeans}}^2$ (6.5), and

$$|\mathbf{k}|_{\text{Jeans}}^2 \approx \chi \left(\frac{m}{m_{\text{pl}}} \right)^2 \frac{(Ha)^2}{v_s^2}; \quad \chi \left(\frac{m}{m_{\text{pl}}} \right)^2 < 1, \quad (6.6)$$

where the Jeans instability occurs.

6.2.1 Subhorizon stable modes and dark-matter acoustic waves

For short-wavelength modes $|\mathbf{k}|_\Delta^2 > |\mathbf{k}|_{\text{Jeans}}^2$, the pressure terms ($v_s^2|\mathbf{k}|^2/a^2$) are dominant in the frequency ω_Δ^2 (2.21), compared with the gravitational attraction $4\pi G\rho_M^H$ of pair-density perturbations. Equation (6.2) for the pair-density perturbation approximately becomes

$$\ddot{\Delta}_M^{\mathbf{k}} + 2H\dot{\Delta}_M^{\mathbf{k}} = -(v_s^2|\mathbf{k}|^2/a^2)\Delta_M^{\mathbf{k}}, \quad (6.7)$$

which is the typical Mukhanov-Sasaki equation, similar to the one for the curvature perturbation. Using Eqs. (3.1), (3.2) and (3.3), we find its solution

$$\Delta_M^{\mathbf{k}}(t) \propto e^{-Ht} \exp -i\tilde{\omega}_\Delta(|\mathbf{k}|)(1 - \zeta^2)^{1/2}t, \quad \zeta \approx \frac{H}{\tilde{\omega}_\Delta(|\mathbf{k}|)} = \frac{Ha}{v_s|\mathbf{k}|_\Delta}, \quad (6.8)$$

where the acoustic wave frequency $\tilde{\omega}_\Delta(|\mathbf{k}|) = v_s|\mathbf{k}|_\Delta/a$.

For the given comoving horizon (Ha) and the sound velocity v_s , the horizon crossing wavenumber $|\mathbf{k}|_{\Delta\text{cross}} = 2Ha/v_s$ (6.4) is larger than the Jeans wavenumber $|\mathbf{k}|_{\text{Jeans}}$ (6.6),

$$|\mathbf{k}|_{\Delta\text{cross}} > |\mathbf{k}|_{\text{Jeans}}. \quad (6.9)$$

This shows that the pair-density perturbations $\Delta_M^{\mathbf{k}}$ oscillate as

- (i) *sub-horizon sized modes*: an underdamped acoustic wave inside the horizon for $\zeta < 1$ and $|\mathbf{k}|_{\Delta} > |\mathbf{k}|_{\Delta\text{cross}} > |\mathbf{k}|_{\text{Jeans}}$, the modes $\Delta_M^{\mathbf{k}}(t)$ are stable acoustic waves;
- (ii) *super-horizon sized modes*: an overdamped acoustic wave outside the horizon for $\zeta > 1$ and $|\mathbf{k}|_{\Delta\text{cross}} > |\mathbf{k}|_{\Delta} > |\mathbf{k}|_{\text{Jeans}}$, the mode amplitudes $\Delta_M^{\mathbf{k}} \propto \text{const}$ are frozen.

On the other hand, as the comoving horizon (Ha) increases and the sound velocity v_s decreases in the pre-inflation epoch, the horizon crossing wavenumber $|\mathbf{k}|_{\Delta\text{cross}}$ (6.4) increases. The acoustic wave modes $\Delta_M^{\mathbf{k}}$ of a fixed wavenumber $|\mathbf{k}|_{\Delta}$ evolve from *subhorizon* to *superhorizon*, and the horizon crossing occurs at $|\mathbf{k}|_{\Delta} = |\mathbf{k}|_{\Delta\text{cross}}$ (6.4).

Moreover, the *super-horizon sized mode* $|\mathbf{k}|_{\Delta}$ reenters the horizon at the horizon $(Ha)_{\text{reenter}}$ and becomes a *sub-horizon sized mode*, when

$$|\mathbf{k}|_{\Delta} = (Ha)_{\text{reenter}}, \quad (6.10)$$

where $(Ha)_{\text{reenter}}^{-1}$ is the comoving horizon size after the recombination. Such mode $|\mathbf{k}|_{\Delta} = (Ha)_{\text{reenter}}$ behaves as an acoustic wave of the dark-matter density perturbations. It imprints on the matter power spectrum of low- ℓ multipoles $\ell \leq 2$, corresponding to large length scales. It is reminiscent of baryon acoustic oscillations due to the coupling in the baryon-photon fluid.

These are qualitative discussions on dark-matter acoustic waves. We expect they to be possibly relevant for observations. However, the quantitative results depend not only on the initial amplitude value $\Delta_M^{\mathbf{k}}(0)$, the wavenumber $|\mathbf{k}|_{\Delta}$ and the horizon crossing size $(Ha)_{\text{cross}}$, but also on the sound velocity v_s in Eq. (6.8).

6.2.2 Unstable superhorizon modes and large-scale structure

For long-wavelength modes $|\mathbf{k}|_{\Delta}^2 \ll |\mathbf{k}|_{\text{Jeans}}^2$, the pressure terms ($v_s^2|\mathbf{k}|^2/a^2$) are negligible in the frequency ω_{Δ}^2 (2.21), compared with the gravitational attraction $4\pi G\rho_M^H$ of pair-density perturbations. Equation (6.2) for the pair-density perturbation approximately becomes

$$\ddot{\Delta}_M^{\mathbf{k}} + 2H\dot{\Delta}_M^{\mathbf{k}} = \chi\left(\frac{m}{m_{\text{pl}}}\right)^2 H^2\Delta_M^{\mathbf{k}}, \quad (6.11)$$

as the microscopic physics (e.g., pressure terms ($v_s^2|\mathbf{k}|^2/a^2$)) is impotent and negligible. The Hubble rate H is approximately a constant, slowly varies in the pre-inflation epoch.

Equation (6.11) is a new kind of differential equation for perturbations, differently from Eq. (6.7) of the Mukhanov-Sasaki type. This equation (6.11) has two independent solutions:

$$\Delta_M^{\mathbf{k}}(t) \propto \exp -2Ht; \quad \Delta_M^{\mathbf{k}}(t) \propto \exp + \frac{\chi H}{2} \left(\frac{m}{m_{\text{pl}}}\right)^2 t. \quad (6.12)$$

At late times, the exponentially glowing modes of pair-density perturbations are crucial. Whereas the exponentially decaying modes physically correspond to those modes with initial overdensity and velocity arranged so that the initial velocity perturbation eventually eases pair-density perturbations.

Equation (6.6) shows that $|\mathbf{k}|_{\Delta}^2 \ll |\mathbf{k}|_{\text{Jeans}}^2$ means $|\mathbf{k}|_{\Delta}^2 < |\mathbf{k}|_{\Delta\text{cross}}^2$, indicating these modes (6.12) are superhorizon size. It is consistent with neglecting the pressure term ($v_s^2|\mathbf{k}|^2/a^2$) of the microscopic physics that cannot causally arrange the pair-density perturbations in superhorizon size. As a result, the pressure terms do not balance the gravitational attraction, leading to an increase in the amplitudes of pair-density perturbations. These unstable and superhorizon-sized modes (6.12) exponentially glow in time. Its characteristic time scale is given by the second solution in Eq. (6.12)

$$\tau_{\Delta}^{-1} = \frac{\chi H}{2} \left(\frac{m}{m_{\text{pl}}} \right)^2. \quad (6.13)$$

These solutions (modes) very differ from the superhorizon-sized modes of frozen constant amplitudes (3.3) or (6.8) for $\zeta \gg 1$. We further study such an unstable and superhorizon-sized mode of fixed wavenumber $|\mathbf{k}|_{\Delta}$ that is in the range

$$|\mathbf{k}|_{\text{Jeans}} > |\mathbf{k}|_{\Delta} > k^*, \quad (6.14)$$

where $|\mathbf{k}|_{\Delta\text{cross}} > |\mathbf{k}|_{\text{Jeans}}$ (6.9) and k^* is the pivot scale of CMB observations. The initial amplitudes $\Delta_M^{\mathbf{k}}(0)$ of such modes (6.12) and (6.14) are very small, as the curvature perturbations. However, they could greatly amplify in the superhorizon before it reenters the subhorizon. Therefore, it is possible that such modes $\Delta_M^{\mathbf{k}}$ of the pair-density perturbation are no longer a small perturbation, when they reenter the horizon and their wavelength $|\mathbf{k}|_{\Delta}^{-1}$ become subhorizon-sized, $|\mathbf{k}|_{\Delta} = (Ha)_{\text{reenter}}$ (6.11). The subhorizon horizon crossing in occurs after the recombination $(Ha)_{\text{reenter}} < (Ha)_*$. As a consequence, this phenomenon can play physical roles in the formations of large-scale structures and galaxy cluster profiles.

We recall the basic scenario of primordial curvature perturbations leading to the large-scale structure in the standard cosmology. The curvature perturbations, whose amplitudes are small constants in superhorizon, reenter the horizon and lead to the CMB temperature anisotropic fluctuation $\delta T/T \sim \mathcal{O}(10^{-5})$. Such fluctuations relate to the matter density perturbations $\delta\rho/\rho \propto \delta T/T$ at the recombination of the redshift $z \sim 10^3$. These matter density perturbations (amplitudes) are small, and their physical sizes (wavelengths) increase linearly as the scale factor $a(t)$. However, under the influence of their gravitational attractions and the Jeans instability, the matter density perturbations glow $\delta\rho/\rho \propto \mathcal{O}(1)$ and become nonlinear, therefore approximately maintain constant physical sizes, eventually forming a large-scale structure.

Our qualitative analysis and discussions show the following alternative possibility. The unstable pair-density perturbations' (6.14), i.e., the dark matter acoustic waves', amplitudes can get amplification in the superhorizon up to the order of unity $\Delta_M^{\mathbf{k}} \propto \mathcal{O}(1)$, when they reenter the horizon after the recombination. Therefore, they should have some physical consequences on the formation of large-scale structure and galaxies' profiles. However, we are not able to give quantitative results in this article and further studies are required.

6.3 Particle-antiparticle density perturbations and “plasma” acoustic wave

We turn to the discussions of the particle-antiparticle density perturbations $\delta_M^{\mathbf{k}}$, described by the frequency $\omega_\delta(\mathbf{k})$ (2.20) and oscillating equation (6.1),

$$\ddot{\delta}_M^{\mathbf{k}} + 2H\dot{\delta}_M^{\mathbf{k}} = -(v_s^2|\mathbf{k}|^2/a^2)\delta_M^{\mathbf{k}}, \quad (6.15)$$

and horizon crossing (6.4). These are the same as those for the pair-density perturbations $\Delta_M^{\mathbf{k}}$, except the absence of the gravitational attraction term $4\pi G\rho_M^H$ and Jeans instability. The solution is similar to the stable $\Delta_M^{\mathbf{k}}$ modes (6.8)

$$\delta_M^{\mathbf{k}}(t) \propto e^{-Ht} \exp -i\tilde{\omega}_\delta(|\mathbf{k}|)(1 - \zeta^2)^{1/2}t, \quad \zeta \approx \frac{H}{\tilde{\omega}_\delta(|\mathbf{k}|)} = \frac{Ha}{v_s|\mathbf{k}|_\delta}, \quad (6.16)$$

where the acoustic wave frequency $\tilde{\omega}_\delta(|\mathbf{k}|) = v_s|\mathbf{k}|_\delta/a$. For the given comoving horizon (Ha) and the sound velocity v_s , the horizon crossing wavenumber $|\mathbf{k}|_{\delta\text{cross}} = 2Ha/v_s$ (6.3). This shows that the particle-antiparticle density perturbations $\delta_M^{\mathbf{k}}$ oscillate as

- (i) *sub-horizon sized modes*: an underdamped acoustic wave mode inside the horizon for $\zeta < 1$ and $|\mathbf{k}|_\delta > |\mathbf{k}|_{\delta\text{cross}}$, the modes $\delta_M^{\mathbf{k}}(t)$ are stable acoustic wave modes;
- (ii) *super-horizon sized modes*: an overdamped acoustic wave mode outside the horizon for $\zeta > 1$ and $|\mathbf{k}|_\delta < |\mathbf{k}|_{\delta\text{cross}}$, the mode amplitudes $\delta_M^{\mathbf{k}} \propto \text{const}$ are frozen.

On the other hand, as the comoving horizon (Ha) increases and the sound velocity v_s decreases in the pre-inflation epoch, the horizon crossing wavenumber $|\mathbf{k}|_{\delta\text{cross}}$ (6.3) increases. The mode $\delta_M^{\mathbf{k}}$ of a fixed wavenumber $|\mathbf{k}|_\delta$ evolves from a *sub-horizon sized mode* to a *super-horizon sized mode*, and the horizon crossing occurs at $|\mathbf{k}|_\delta = |\mathbf{k}|_{\delta\text{cross}}$ (6.3). Moreover, the *super-horizon sized mode* $|\mathbf{k}|_\delta$ reenters the horizon at the horizon $(Ha)_{\text{reenter}}$, when

$$|\mathbf{k}|_\delta = (Ha)_{\text{reenter}}, \quad (6.17)$$

after the recombination. It becomes a *sub-horizon sized mode* again.

The modes $|\mathbf{k}|_\delta = (Ha)_{\text{reenter}}$ of the particle-antiparticle density perturbations $\delta_M^{\mathbf{k}}$ (2.13) represent the acoustic waves of particle and antiparticle oscillations of the dispersion relation (2.20). They are analogous to the neutral plasma oscillations of electrons and positrons. They respect the symmetry of particles and antiparticles. These modes exit the horizon in the pre-inflation epoch and reenter the horizon after the recombination. It implies that such acoustic waves from the primordial Universe would leave their imprints on the Universe after the recombination, possibly imprinting on the matter power spectrum of low- ℓ multipoles $\ell \leq 2$, corresponding to large length scales. However, we expect that the mode amplitudes $\delta_M^{\mathbf{k}}$ should be small, given the energy densities ρ_M^+ and ρ_M^- of particles and antiparticles are small. Namely the pair energy densities $\rho_M^H \approx \rho_M^+ + \rho_M^-$ and $\rho_M^+ \approx \rho_M^-$ are small in the pre-inflation epoch.

In this section, we qualitatively describe three types of “dark-matter” acoustic waves originated from the particle-antiparticle oscillations in the pre-inflation epoch:

(i) stable subhorizon pair-density perturbations; (ii) unstable superhorizon pair-density perturbations; (iii) particle-antiparticle density perturbations. We present some discussions on their returns to the horizon after the recombination and possible relevance for observations. However, we cannot give quantitative results that depend not only on the perturbation modes' wavenumbers $|\mathbf{k}|_{\Delta,\delta}$, initial amplitude values $\Delta_M^{\mathbf{k}}(0)$ and $\delta_M^{\mathbf{k}}(0)$, and the sound velocity v_s in their oscillating equations (6.7) and (6.15), but also on the horizon crossing size $(Ha)^{-1}$ (6.3) and (6.4).

7 Summary and remarks

The article presents studies of baryogenesis, magnetogenesis, and dark-matter acoustic waves in the scenario $\tilde{\Lambda}$ CDM. We summarize the lengthy article by briefly summarising the fundamental equations adopted, basic physical phenomena described and results obtained that give some insight into these three issues.

We study the perturbations of particle and antiparticle densities in the holographic and massive pair plasma state in the reheating. Starting from Eqs. (2.1-2.4) for the density perturbations of particles and antiparticles, we derive the acoustic wave equations (2.18-2.19) for the particle-antiparticle symmetric pair-density perturbation Δ_M (2.12) and the particle-antiparticle asymmetric density perturbation δ_M (2.13). We study the oscillating behaviours of the lowest-lying modes of zero wavenumbers $|\mathbf{k}|_{\Delta,\delta} = 0$. We show that they evolve from superhorizon to subhorizon (4.2) in the preheating episode and from subhorizon to superhorizon (4.7) in the genuine reheating episode. In the latter case, δ_M undergoes horizon crossing to generate the net number density (4.13) of particle and antiparticle, leading to the baryogenesis phenomenon. We obtain the baryon number-to-entropy ratio (5.3) consistent with observations. Moreover, the magnetogenesis phenomenon occurs, attributed to the net electric current produced by baryogenesis. From purely theoretical viewpoints of the scenario, we estimate the lower and upper bounds of primordial magnetic fields. The results are consistent with the current observational constraints.

In addition, we study the acoustic wave-propagating modes ($|\mathbf{k}|_{\Delta,\delta} \neq 0$) of the pair-density perturbation $\Delta_M^{\mathbf{k}}$ (6.2) and the particle-antiparticle asymmetric density perturbation $\delta_M^{\mathbf{k}}$ (6.1). They represent the dark-matter acoustic waves. We show how they become superhorizon-sized modes (6.3) and (6.4) in the pre-inflation epoch, then return to the horizon $|\mathbf{k}|_{\Delta,\delta} = (Ha)_{\text{reenter}}$ after the recombination. These modes can behave as stable acoustic waves of dark matter density perturbations. They possibly imprint on the matter power spectrum of low- ℓ multipoles $\ell \leq 2$, corresponding to large-length scales. Due to the Jeans instability of the pair-density perturbation $\Delta_M^{\mathbf{k}}$ (6.11), the tiny amplitudes $\Delta_M^{\mathbf{k}} \ll \mathcal{O}(1)$ of unstable superhorizon sized modes can get amplified. When they reenter the horizon after the recombination, these modes of pair-density perturbations can be of the order of unity $\Delta_M^{\mathbf{k}} \propto \mathcal{O}(1)$. As a consequence, they should have some physical influences on forming large-scale structures and galaxy cluster profiles. It would be worthwhile to study whether these Jeans-amplified pair-density perturbations $\Delta_M^{\mathbf{k}}$ produce primordial gravitational waves when they reenter the horizon.

Further studies are required and more elaborately numerical computations are needed. Nevertheless, we expect the theoretical scenario and results to provide some insights into the baryogenesis and magnetogenesis, the dark matter acoustic waves and their impacts on the Universe's evolution and structure.

References

- [1] A. A. Starobinsky, *A new type of isotropic cosmological models without singularity*, *Phys. Lett. B* **91** (1980) 99.
- [2] A. H. Guth, *The inflationary universe: A possible solution to the horizon and flatness problems*, *Phys. Rev. D* **23** (1981) 347.
- [3] A. D. Linde, *A new inflationary universe scenario: A possible solution of the horizon, flatness, homogeneity, isotropy and primordial monopole problems*, *Phys. Lett. B* **108** (1982) 389–393.
- [4] V. F. Mukhanov and G. V. Chibisov, *The vacuum energy and large scale structure of the universe*, *Sov. Phys. JETP* **56** (1982) 258–265.
- [5] A. Albrecht and P. J. Steinhardt, *Cosmology for grand unified theories with radiatively induced symmetry breaking*, *Phys. Rev. Lett.* **48** (1982) 1220.
- [6] A. D. Linde, *Chaotic inflation*, *Phys. Lett. B* **129** (1983) 177.
- [7] R. Kallosh and A. Linde, *BICEP/Keck and cosmological attractors*, *JCAP* **12** (2021) 008 [[2110.10902](#)].
- [8] L. Kofman, A. D. Linde and A. A. Starobinsky, *Reheating after inflation*, *Phys. Rev. Lett.* **73** (1994) 3195 [[hep-th/9405187](#)].
- [9] L. Kofman, A. D. Linde and A. A. Starobinsky, *Towards the theory of reheating after inflation*, *Phys. Rev. D* **56** (1997) 3258 [[hep-ph/9704452](#)].
- [10] Y. Shtanov, J. H. Traschen and R. H. Brandenberger, *Universe reheating after inflation*, *Phys. Rev. D* **51** (1995) 5438 [[hep-ph/9407247](#)].
- [11] B. A. Bassett and S. Liberati, *Geometric reheating after inflation*, *Phys. Rev. D* **58** (1998) 021302 [[hep-ph/9709417](#)].
- [12] S. Tsujikawa, K.-i. Maeda and T. Torii, *Resonant particle production with nonminimally coupled scalar fields in preheating after inflation*, *Phys. Rev. D* **60** (1999) 063515 [[hep-ph/9901306](#)].
- [13] D. I. Podolsky and A. A. Starobinsky, *Chaotic reheating*, *Grav. Cosmol. Suppl.* **8N1** (2002) 13 [[astro-ph/0204327](#)].
- [14] R. Allahverdi, R. Brandenberger, F.-Y. Cyr-Racine and A. Mazumdar, *Reheating in inflationary cosmology: Theory and applications*, *Ann. Rev. Nucl. Part. Sci.* **60** (2010) 27 [[1001.2600](#)].

- [15] M. A. Amin, R. Easther, H. Finkel, R. Flauger and M. P. Hertzberg, *Oscillons after inflation*, *Phys. Rev. Lett.* **108** (2012) 241302 [[1106.3335](#)].
- [16] M. A. Amin, M. P. Hertzberg, D. I. Kaiser and J. Karouby, *Nonperturbative dynamics of reheating after inflation: A review*, *Int. J. Mod. Phys. D* **24** (2014) 1530003 [[1410.3808](#)].
- [17] P. Adshead, J. T. Giblin, M. Pieroni and Z. J. Weiner, *Constraining axion inflation with gravitational waves across 29 decades in frequency*, *Phys. Rev. Lett.* **124** (2020) 171301 [[1909.12843](#)].
- [18] PLANCK collaboration, *Planck 2015 results. xiii. cosmological parameters*, *Astron. Astrophys.* **594** (2016) A13 [[1502.01589](#)].
- [19] A. D. Dolgov and A. D. Linde, *Baryon asymmetry in inflationary universe*, *Phys. Lett. B* **116** (1982) 329.
- [20] L. F. Abbott, E. Farhi and M. B. Wise, *Particle production in the new inflationary cosmology*, *Phys. Lett. B* **117** (1982) 29.
- [21] V. A. Kuzmin, V. A. Rubakov and M. E. Shaposhnikov, *On the anomalous electroweak baryon number nonconservation in the early universe*, *Phys. Lett. B* **155** (1985) 36.
- [22] M. Dine and A. Kusenko, *The origin of the matter - antimatter asymmetry*, *Rev. Mod. Phys.* **76** (2003) 1 [[hep-ph/0303065](#)].
- [23] A. Dolgov and K. Freese, *Calculation of particle production by Nambu Goldstone bosons with application to inflation reheating and baryogenesis*, *Phys. Rev. D* **51** (1995) 2693 [[hep-ph/9410346](#)].
- [24] A. Dolgov, K. Freese, R. Rangarajan and M. Srednicki, *Baryogenesis during reheating in natural inflation and comments on spontaneous baryogenesis*, *Phys. Rev. D* **56** (1997) 6155 [[hep-ph/9610405](#)].
- [25] J. Garcia-Bellido, D. Y. Grigoriev, A. Kusenko and M. E. Shaposhnikov, *Nonequilibrium electroweak baryogenesis from preheating after inflation*, *Phys. Rev. D* **60** (1999) 123504 [[hep-ph/9902449](#)].
- [26] S. Davidson, M. Losada and A. Riotto, *A new perspective on baryogenesis*, *Phys. Rev. Lett.* **84** (2000) 4284 [[hep-ph/0001301](#)].
- [27] A. Megevand, *Effect of reheating on electroweak baryogenesis*, *Phys. Rev. D* **64** (2001) 027303 [[hep-ph/0011019](#)].
- [28] A. Tranberg and J. Smit, *Baryon asymmetry from electroweak tachyonic preheating*, *JHEP* **11** (2003) 016 [[hep-ph/0310342](#)].
- [29] A. Tranberg and J. Smit, *Simulations of cold electroweak baryogenesis: Dependence on Higgs mass and strength of cp -violation*, *JHEP* **08** (2006) 012 [[hep-ph/0604263](#)].
- [30] M. P. Hertzberg and J. Karouby, *Generating the observed baryon asymmetry from the inflaton field*, *Phys. Rev. D* **89** (2014) 063523 [[1309.0010](#)].

- [31] M. P. Hertzberg and J. Karouby, *Baryogenesis from the inflaton field*, *Phys. Lett. B* **737** (2014) 34 [[1309.0007](#)].
- [32] M. P. Hertzberg, J. Karouby, W. G. Spitzer, J. C. Becerra and L. Li, *Theory of self-resonance after inflation. ii. quantum mechanics and particle-antiparticle asymmetry*, *Phys. Rev. D* **90** (2014) 123529 [[1408.1398](#)].
- [33] K. D. Lozanov and M. A. Amin, *End of inflation, oscillons, and matter-antimatter asymmetry*, *Phys. Rev. D* **90** (2014) 083528 [[1408.1811](#)].
- [34] K. M. Zurek, *Asymmetric dark matter: Theories, signatures, and constraints*, *Phys. Rept.* **537** (2014) 91 [[1308.0338](#)].
- [35] A. Kandus, K. E. Kunze and C. G. Tsagas, *Primordial magnetogenesis*, *Phys. Rept.* **505** (2011) 1 [[1007.3891](#)].
- [36] PLANCK collaboration, *Planck 2015 results. XIX. constraints on primordial magnetic fields*, *Astron. Astrophys.* **594** (2016) A19 [[1502.01594](#)].
- [37] P. P. Kronberg, *Extragalactic magnetic fields*, *Rept. Prog. Phys.* **57** (1994) 325.
- [38] A. Diaz-Gil, J. Garcia-Bellido, M. Garcia Perez and A. Gonzalez-Arroyo, *Magnetic field production during preheating at the electroweak scale*, *Phys. Rev. Lett.* **100** (2008) 241301 [[0712.4263](#)].
- [39] A. Diaz-Gil, J. Garcia-Bellido, M. Garcia Perez and A. Gonzalez-Arroyo, *Primordial magnetic fields from preheating at the electroweak scale*, *JHEP* **07** (2008) 043 [[0805.4159](#)].
- [40] D. Grasso and H. R. Rubinstein, *Magnetic fields in the early universe*, *Phys. Rept.* **348** (2001) 163 [[astro-ph/0009061](#)].
- [41] K. Subramanian, *The origin, evolution and signatures of primordial magnetic fields*, *Rept. Prog. Phys.* **79** (2016) 076901 [[1504.02311](#)].
- [42] S.-S. Xue, *How universe evolves with cosmological and gravitational constants*, *Nucl. Phys. B* **897** (2015) 326 [[1410.6152](#)].
- [43] L. Parker and S. A. Fulling, *Quantized matter fields and the avoidance of singularities in general relativity*, *Phys. Rev. D* **7** (1973) 2357.
- [44] S.-S. Xue, *Massive particle pair production and oscillation in Friedman universe: its effect on inflation*, *Eur. Phys. J. C* **83** (2023) 36 [[2112.09661](#)].
- [45] S.-S. Xue, *Massive particle pair production and oscillation in Friedman universe: reheating energy and entropy, and cold dark matter, to appear on Eur. Phys. J. C* (2023) [[2006.15622](#)].
- [46] E. W. Kolb and M. S. Turner, *The Early Universe*, vol. 69. Westview Press, A member of the Perseus Books Group, 1990, [10.1201/9780429492860](#).

- [47] J. J. Sakurai and J. Napolitano, *Modern quantum mechanics*. Cambridge: Cambridge University Press, 3rd revised edition ed., 2020, [10.1017/9781108587280](https://doi.org/10.1017/9781108587280).
- [48] L. Landau and E. Lifshiz, *Quantum Mechanics (Non-relativistic Theory)*. Elsevier Butterworth-Heinemann, 1977.
- [49] S. Hollands and R. M. Wald, *An alternative to inflation*, *Gen. Rel. Grav.* **34** (2002) 2043 [[gr-qc/0205058](https://arxiv.org/abs/gr-qc/0205058)].
- [50] S.-S. Xue, *Cosmological Λ driven inflation and produced massive particles*, [1910.03938](https://arxiv.org/abs/1910.03938).
- [51] S.-S. Xue, *Cosmological constant, matter, cosmic inflation and coincidence*, *Mod. Phys. Lett. A* **35** (2020) 2050123 [[2004.10859](https://arxiv.org/abs/2004.10859)].
- [52] J. Mielczarek, *Reheating temperature from the CMB*, *Phys. Rev. D* **83** (2011) 023502 [[1009.2359](https://arxiv.org/abs/1009.2359)].
- [53] A. D. Sakharov, *Violation of CP invariance, C asymmetry, and baryon asymmetry of the universe*, *Soviet Journal of Experimental and Theoretical Physics Letters* **5** (1967) 24.
- [54] S.-S. Xue, *Massive particle pair production and oscillation in Friedman universe: dark energy and matter interaction*, [2203.11918](https://arxiv.org/abs/2203.11918).